in response to a HFD to investigate the role of Rho–Rho-kinase signaling in obesity, instead of a genetic model of obesity involving leptin receptor deficiency. We found increased Rho-kinase activity in the adipose tissue of obese mice fed a HFD compared with that in mice fed a LFD. In vitro studies of long-term cultures of adipocytes, as a model of adipocytes in the obese state (*15*), and subfractionation of the adipose tissue of obese mice, revealed that Rho-kinase activation in adipose tissue occurred mainly in adipocytes. Systemic administration of the Rho-kinase inhibitor fasudil blocked activation of Rho-kinase in adipose tissue and attenuated various effects of a HFD in mice, including weight gain, systemic insulin resistance, adipocyte hypertrophy, inflammatory cell infiltration of adipose tissue, and dysregulation of adipocytokine expression. These findings indicate that Rho–Rho-kinase signaling plays a pivotal role in obesity and in the development of obesity-related disorders.

To identify the effects of Rho–Rho-kinase signaling in adipose tissue, we produced transgenic mice that specifically expressed DN-RhoA in adipocytes. Analyses of these mice revealed that specific inhibition of Rho-kinase signaling in adipose tissue inhibited HFD-induced adiposity and weight gain. It also attenuated several metabolic abnormalities associated with obesity induced by a HFD. This implicates activation of this pathway in the adipose tissue as a culprit in the initiation of HFD-induced obesity and obesity-related metabolic disturbances. Several mechanisms likely

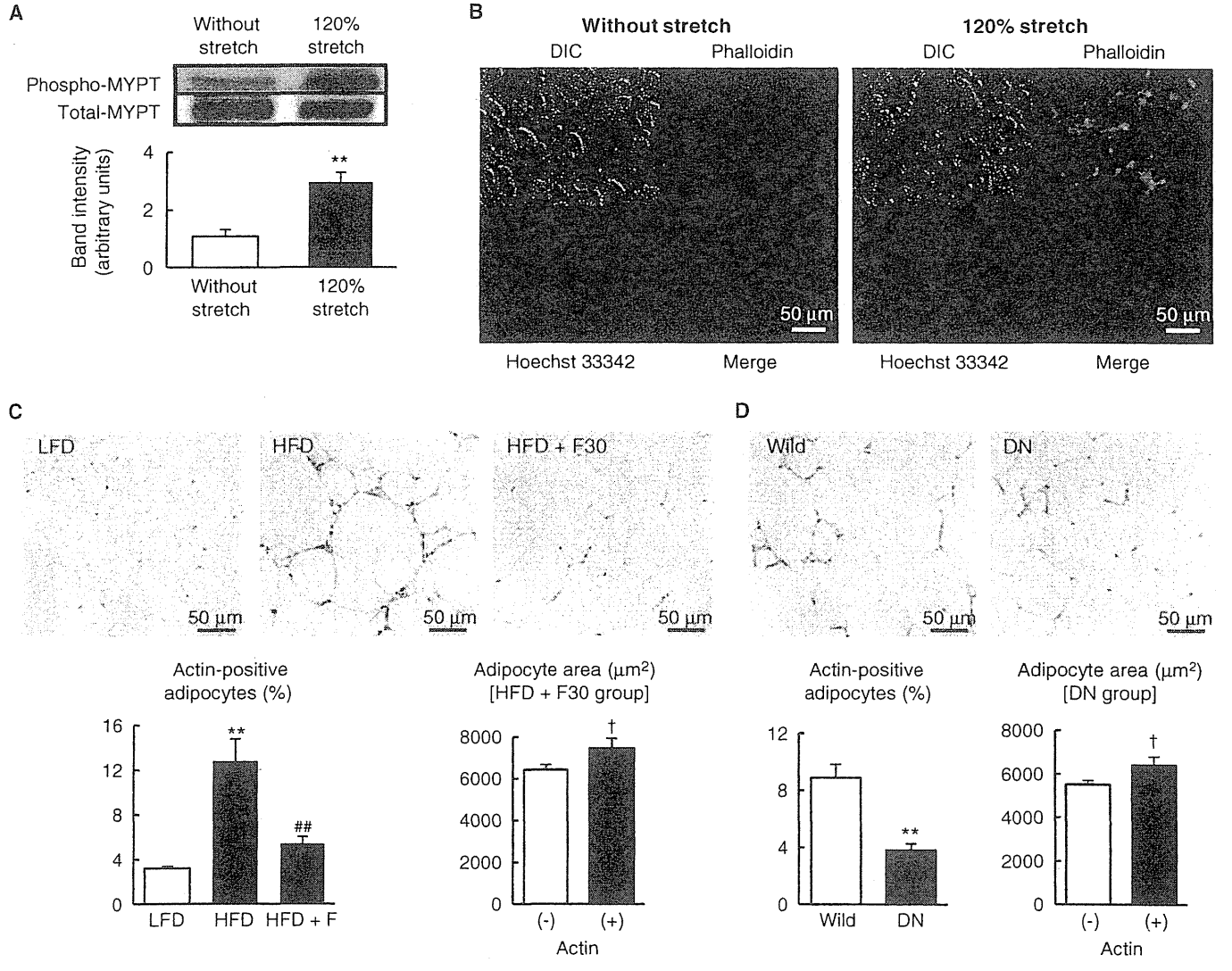

Fig. 5. Mechanical stretch elicited Rho-kinase activity and stress fiber formation in mature adipocytes. (A) Rho-kinase activity was evaluated by immunoblot for phospho-MYPT. $^{**}P < 0.01$ versus without stretch. $n = 4$. (B) Stress fiber formation was detected by rhodamine-labeled phalloidin staining. Nuclear staining was contrasted with stress fiber staining using Hoechst 33342 dye. DIC, differential interference contrast. (C) Actin staining in adipose tissue of mice fed a LFD, obese mice fed a HFD, and fasudil-treated mice fed a HFD. The lower left panel provides quantification, giving the percentage of actin-positive adipocytes. The lower right panel provides the size of actin-positive and -negative adipocytes in the HFD + F30 group. $^{**}P < 0.01$ versus LFD, $^{\#\#}P < 0.01$ versus HFD. $n = 4$. $^{\dagger}P < 0.05$ versus actin-negative adipocytes. $n = 4$. (D) Actin staining in adipose tissue in DN-RhoA TG and wild-type mice. The lower left panel provides quantification. The lower right panel provides the size of actin-positive and -negative adipocytes in the DN group. $^{**}P < 0.01$ versus wild type, $n = 4$. $^{\dagger}P < 0.05$ versus actin-negative adipocytes, $n = 4$.

contributed to the improved glucose metabolism in DN-RhoA TG mice (Fig. 3B). Changes in adipocytokine expression produced by a HFD were partially reversed in DN-RhoA TG mice in a direction that would tend to enhance insulin sensitivity (*16*), as was indeed observed. Increased insulin sensitivity in adipose tissues, as well as the decrease in circulating free fatty acids (Fig. 3C), would also contribute to improved glucose metabolism. DN-RhoA was under the control of the aP2 promoter, which is also expressed in macrophages, lung epithelial cells, and parts of the brain (*17–19*). Therefore, it is conceivable that the changes in adipose tissue phenotype we observed resulted from decreased activation of Rho-kinase in macrophages infiltrating adipose tissues or from alterations in neuronal regulation of adipose tissue. However, Rho-kinase activation in macrophages in HFD-fed obese mice was marginal (Fig. 1G), indicating that the effects of blocking this activation would be limited. Furthermore, any changes in Rho-kinase activity in the central nervous system did not appear to affect appetite or satiety, because food intake between wild-type and DN-RhoA TG mice was similar (wild type, 1.95 ± 0.22 g/day; DN-RhoA TG, 1.86 ± 0.19 g/day). Therefore, we do not consider inhibition of Rho–Rho-kinase pathway in these systems functionally relevant to the obese phenotype in our DN-RhoA TG mice.

DN-RhoA TG mice fed a HFD were leaner than wild-type controls, suggesting the possibility that the reversal of the aberrant HFD-induced adipose tissue phenotype might be secondary to decrease in weight. However, a fasudil dosage of 3 mg/kg per day, which did not affect body weight, attenuated metabolic abnormalities and the aberrant phenotype of adipose tissues in HFD-fed mice (Fig. 1). Similarly, DN-RhoA TG mice were more sensitive to insulin than wild-type mice at a time point when body weight did not differ (Fig. 3, G and H). Thus, we conclude that activation of Rho–Rho-kinase pathway in adipocytes is a culprit in the pernicious phenotype of diet-induced obesity.

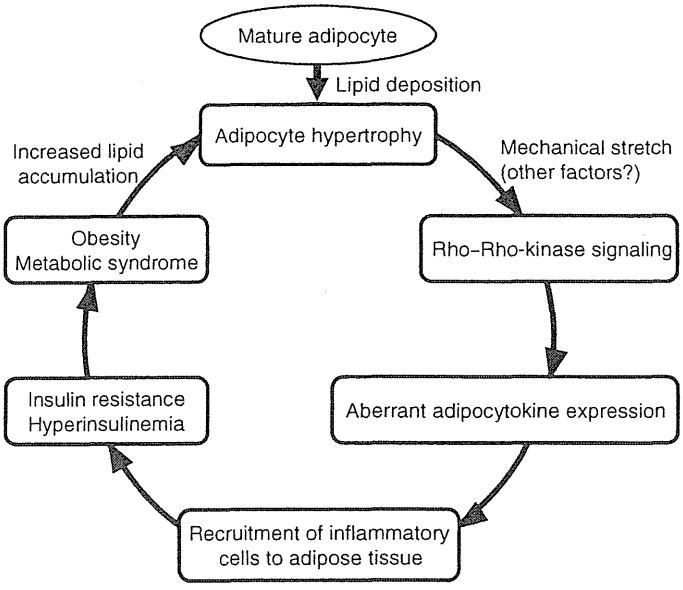

Fig. 6. Schema depicting the vicious cycle of adipose tissues in obesity. After adipocytes mature, increasing lipid accumulation leads to their hypertrophy and consequently to mechanical stretch. Mechanical stretch (and possibly additional factors) promotes Rho-kinase activity, which contributes to aberrant expression of adipocytokines. The acquisition of the hypertrophic phenotype and abnormal adipocytokine secretion, in turn, accelerate inflammation of adipose tissue by inflammatory cells, leading to systemic insulin resistance. Insulin resistance cumulates in obesity and its related pathologies, which further induce adipocyte hypertrophy. This vicious cycle contributes to the initiation and progression of obesity and obesity-related systemic diseases.

What triggers the activation of Rho–Rho-kinase signaling in adipocytes of obese mice? Our data support the hypothesis that mechanical stress caused by hypertrophic change triggers activation of the Rho–Rho-kinase pathway. In obesity, adipocytes are affected by various stresses, including those associated with the state of inflammation caused by the infiltration of inflammatory cells (*20*). Adipocytes undergo an extreme increase in volume in obese subjects (*21*), indicating that they are subjected to hypertrophic stress during the accumulation of fat depots. Here, we showed that mechanical stretch comparable to that elicited by hypertrophy induces the activation of Rho–Rho-kinase signaling. Mechanical stretch might not be the only signal that induces Rho–Rho-kinase activity in hypertrophic adipocytes. For instance, increased insulin concentrations or oxidative stress might also activate Rho signaling. However, we observed similar phenotypic changes in in vitro stretched adipocytes and in vivo hypertrophic adipocytes with similar increases in adipocyte size. These findings, although indirect, indicate that phenotype alteration of hypertrophic adipocytes in vivo may be induced, at least in part, by mechanical stress. Indeed, similar functional alterations in response to mechanical stretch have been shown in other cell types, including VSMCs and endothelial cells (*22*). Demonstration of a direct link between mechanical stress in adipocytes and the progression of obesity-related disorders warrants further investigations.

Activation of Rho–Rho-kinase signaling is critical for cytokine expression in adipocytes. A recent study demonstrated that adipocytokine expression, including that of MCP-1 and plasminogen activator inhibitor type 1 (PAI-1), was increased by Rho–Rho-kinase signaling in cultured adipocytes through activation of nuclear factor κB (NF-κB), a master regulator of cytokine gene expression (*12*, *23*). MCP-1 is also directly regulated by Rho-kinase, as observed in VSMCs (*24*). We propose that, in hypertrophic adipocytes, activation of Rho–Rho-kinase signaling through mechanical stress induces *TNFα* expression—likely through the activation of NF-κB—and also induces *MCP-1* expression, leading to macrophage infiltration into adipose tissue. This enhances inflammatory changes in adipose tissue and aggravates systemic metabolic disturbances including hyperinsulinemia, which inhibits adipocyte lipolysis, leading to additional adipocyte hypertrophy. These events establish a vicious circle culminating in the progression of obesity (Fig. 6). Our data provide evidence for a role of hypertrophic stress in the inflammatory changes that take place in adipose tissue.

The activation of Rho-kinase by Rho inhibits adipogenesis from mesenchymal precursor cells, and Rho activation is suppressed during mesenchymal cell commitment into the adipocyte linage (*25*). During adipocyte differentiation, filamentous actin is converted from long stress fibers to cortical actin. These changes are paralleled by suppression of the ROCK2 isoform of Rho-kinase, and treatment with a Rho-kinase inhibitor inhibits cortical stress fiber formation, implying that Rho–Rho-kinase signaling is also suppressed during adipogenesis (*26*). Our data showed that after adipocyte maturation, long-term culture was associated with increased Rho-kinase activity, indicating that adipocytes acquired the aberrant phenotype associated with adipocyte hypertrophy in obesity (Fig. 5). This phenotypic change is important not only in the pathogenesis of the inflammatory response in adipose tissues, but also for adipocyte survival, because stress fiber formation is crucial for the maintenance of cellular structure (*27*). For instance, the vascular endothelial cells that line blood vessels experience fluid shear as blood flows across their surface. This stimulates RhoA activation and the formation of actin stress fibers, which

are believed to help endothelial cells to remain flat under high fluid shear (*28*, *29*). In cardiomyocytes, RhoA activation is required for cytoskeletal organization and protects against apoptosis (*30*). Because adipocytes are under the stress of cellular hypertrophy (*20*), it can be surmised that Rho–Rho-kinase activation is necessary for the maintenance of cell structure. Rho–Rho-kinase signaling in turn leads to the "hypertrophic adipocyte phenotype" and, consequently, inflammatory changes in adipose tissue. We consistently found that in mature adipocytes, the expression of adiponectin, which is involved in systemic insulin sensitivity, was decreased and that of MCP-1, which initiates tissue inflammatory change, was increased by mechanical stress. These changes in mRNA abundance were considered to reflect the phenotypic changes of adipocytes by mechanical stress. Mechanical stress thus serves as an initial trigger to activate the Rho–Rho-kinase pathway and the subsequent alteration of adipocyte phenotype, including reorganization of the cytoskeleton and aberrant cytokine expression. Indeed, we found that the adipocytes of obese mice fed a HFD showed Rho–Rho-kinase–dependent formation of stress fibers (Fig. 5, C and D).

Rho-kinase is indispensable for glucose transport in myocytes and in adipocytes (*31*), and genetic disruption of the ROCK1 isoform of Rho-kinase leads to insulin resistance (*32*), identifying a physiological role for Rho-kinase in glucose utilization. Here and in a previous study, we showed that, in obesity, activation of Rho-kinase in muscle (*11*) or adipose tissue leads to systemic insulin resistance. Together with data implicating ROCK2 in adipocyte development (*26*), our findings indicate that Rho–Rho-kinase signaling plays multiple—sometimes apparently opposing—roles in glucose metabolism under physiological and pathological conditions.

Obesity increases the risk of comorbid conditions, including cardiovascular disease and diabetes, through mechanisms that remain unclear. The degree of abdominal adiposity, as defined by abdominal circumference or by the area of abdominal adipose tissue, appears to be an important marker for the risk of cardiovascular events (*33*). Our data suggest that activation of the Rho–Rho-kinase pathway in adipocytes promotes the acquisition of the aberrant hypertrophic adipocyte phenotype and is crucial for inflammatory changes in adipose tissue. These inflammatory changes accelerate systemic insulin resistance and additional adipocyte hypertrophy (*4*), contributing to the progression of obesity and its related cardiovascular events (Fig. 6). Rho-kinase inhibitors have been used to treat diseases associated with inflammation including asthma (*34*) and rheumatoid arthritis (*35*). Our data suggest that they may also provide a therapeutic strategy against the initiation and progression of metabolic syndrome.

In conclusion, we implicated Rho–Rho-kinase signaling as a culprit in a vicious circle in obesity composed of adipocyte phenotypic changes, inflammation of adipose tissues, and pathological consequences of obesity. Our data demonstrated that the Rho-kinase inhibitor fasudil blocked this vicious cycle and could thus provide a plausible therapeutic strategy for obesity and related systemic disorders, including insulin resistance and atherosclerosis.

MATERIALS AND METHODS

Plasmids and constructs

In constructing the transgenic expression vector, human dominant-negative RhoA mutant (*36*) (DN-RhoA) (provided by K. Kaibuchi, Nagoya University), was ligated with the mouse aP2 promoter (*37*) (provided by BM. Spiegelman, Harvard University). The ligated DN-RhoA complementary DNA (cDNA) was followed by rabbit β-globin (RBG) poly(A) (polyadenylate) tail, and the clone was designated as aP2–DN-RhoA–RBG poly(A) (Fig. 2A).

Generation of transgenic mice that specifically expressed DN-RhoA in adipose tissue

For the generation of adipose tissue–specific DN-RhoA TG mice, we microinjected the Xho I–Not I fragment of aP2–DN-RhoA–RBG poly(A) into one-cell stage fertilized mouse embryos obtained from superovulated C57BL/6J mice (Fig. 2A). Founder mice were identified by Southern blot analysis of genomic DNA with human RhoA cDNA as a probe (Fig. 2B). The positive DN-RhoA TG founders were crossed with wild-type C57BL/6 mice (Charles River Japan Inc.) to obtain the F1 generation. Genomic DNA was isolated from tail biopsies at 3 weeks of age with a DNeasy kit (Qiagen), and screening of genomic DNA samples was done by polymerase chain reaction (PCR) using transgene-specific oligonucleotide primers, TAATACGACTCACTATAGG (aP2 promoter side) and TTCTGGGG-TCCACTTTTCTG (RhoA gene side) (Fig. 2A), which amplify a 1310–base pair (bp) region spanning the junction between the aP2 promoter and the DN-RhoA gene (Fig. 2A). Genomic DNA was isolated from tail biopsies at 3 weeks of age with a DNeasy kit and subjected to Southern blot analysis to identify the transgene. Southern blots were performed with a ^{32}P-labeled probe composed of 1310 bp of aP2–DN-RhoA gene (Fig. 2B). DN-RhoA expression in different founder lines was confirmed by reverse transcription PCR (RT-PCR) using primer sets specific for the DN-RhoA cDNA (table S1 and Fig. 2C).

Animal experimental protocol

Six-week-old male C57BL/6J mice (CLEA Japan Inc.) were divided into four groups (n = 6 per group) and fed a HFD (60% lard, Research Diets Inc.), a LFD (10% lard, Research Diets Inc.), and a HFD with Rho-kinase inhibitor fasudil (Asahi Kasei) at 3 or 30 mg/kg per day (HFD + F3 and HFD + F30, respectively). Fasudil is the Rho-kinase inhibitor most frequently used in long-term in vivo experiments. Its in vivo metabolite, hydroxyfasudil, is more selective for Rho-kinase than the parent drug; the affinity of hydroxyfasudil for Rho-kinase is 100 times higher than for PKC (protein kinase C) and 1000 times higher than for myosin light-chain kinase (*38*–*40*). After 12 weeks on their respective diets, mice were killed and blood samples and epididymal WAT were obtained (*41*). Body weights and tissue weights of the epididymal WAT were also measured. In experiments with adipose tissue–specific DN-RhoA TG mice, TG mice and their wild-type littermates were maintained on HFDs (60% lard) from 6 to 18 weeks of age. Body weight and chow intake were monitored weekly. At 18 weeks of age, mice were killed and epididymal fat tissues were harvested. This study was performed in accordance with the institutional guidelines of the Animal Care and Experimentation Committee in Keio University.

Glucose and insulin tolerance tests

After 12 weeks on their respective diets, mice fed a LFD, HFD, or HFD plus fasudil were subjected to glucose and insulin tolerance tests (GTT and ITT) as described (*42*). Briefly, glucose (1 g/kg) was injected intraperitoneally and blood samples were collected from a tail vein at various time points. Insulin tolerance test was also performed by injecting regular insulin (0.75 IU/kg body weight; Humulin R, Eli Lilly & Co.) intraperitoneally after a 2-hour fast.

Isolation of mature adipocytes and stromal vascular fraction

Isolation of mature adipocytes and stromal vascular fraction was performed as described (*43*). Adipose tissues were harvested and minced in Krebs-Ringer-bicarbonate-Hepes (KRBH) buffer containing 1% (w/v) bovine serum albumin (BSA) (Sigma). Collagenase (Liberase 3, Roche Diagnostics Corp.) was added to a final concentration of 2 mg/ml, and samples were incubated at 37°C on an orbital shaker for 30 min. Samples

were then passed through a 250-μm nylon mesh filter. The suspension was centrifuged at 300*g* for 1 min. Floating cells were collected as the mature adipocyte fraction, and the pelleted cells were collected as the stromal vascular fraction.

Histological analysis and immunohistochemistry

Portions of epididymal adipose tissue were removed and fixed with 10% formaldehyde and embedded in paraffin. Sections were stained with hematoxylin and eosin. For the detection of macrophage infiltration in adipose tissue, immunohistochemistry was performed with F4/80 antibody, which detected macrophage-specific protein (*44*). The number of F4/80-positive cells was counted in a blinded fashion under a microscope with a 400× objective. More than 50 serial fields were examined in each mouse, and five mice were analyzed per group. Stress fibers were detected by rhodamine-labeled phalloidin staining (*45*) or by immunohistochemistry with an anti-actin antibody (Abcam). Adipocyte size was measured with the software Win Roof (Mitani). Adipocyte area was measured by randomly selecting 50 serial fields with a 400× objective for each mouse; five mice were analyzed in each group. To measure the size of acin-positive and actin-negative adipocytes, we randomly selected more than 50 serial fields with a 400× objective of adipose tissue in the HFD + F30 and DN group.

Cell culture protocol

3T3-L1 fibroblasts (European Collection of Cell Cultures) were cultured in Dulbecco's modified Eagle's medium (DMEM) supplemented with 10% (v/v) newborn calf serum and induced to differentiate into adipocytes by exposure for 2 days to induction medium, DMEM containing 0.25 μM dexamethasone (Nacalai Chemicals), 0.5 mM 3-isobutyl-1-methylxanthine (Nacalai), insulin (10 μg/ml; Lilly), and 10% fetal bovine serum (FBS) (day 0). Two days later, the medium was changed to DMEM containing 10% FBS and insulin (10 μg/ml) (day 2). Two days later, media were changed to DMEM containing 10% FBS only (day 4). Subsequently, media were exchanged every other day until day 14. In this protocol, cells become differentiated into mature adipocytes containing fat droplets at day 8 (*46*). After day 8, increased amounts of fat droplet accumulated and cell size increased. To examine the effects of Rho-kinase inhibition on mature adipocytes, we treated the cells with Rho-kinase inhibitors, Y-27632 (10 μM, Calbiochem) and fasudil (10 μM) after day 8. Cells were harvested at days 4, 8, 12, and 16 and analyzed for Rho-kinase activity and adipocytokine mRNA abundance. We used Y-27632 as a Rho-kinase inhibitor in the in vitro experiments because this reagent is more specific than fasudil itself and is widely used for in vitro experiments.

Mechanical stretch of adipocytes

The application of uniaxial stretch to differentiating 3T3-L1 cells was carried out as described (*47*), except static stretching condition was used in this study. Briefly, 3T3-L1 fibroblasts were cultured in collagen-coated silicon chambers and differentiated into mature adipocytes. On day 12, mature adipocytes were subjected to stretch. Cells were subjected to constant stretching of up to 120% of the initial length for a 72-hour duration, conditions that preserve cell survival and the viability of mature adipocytes (*47*). No apparent sign of cell damage, such as detachment of cells from the substratum, was observed under these conditions. Stretched cells were harvested and subjected to real-time PCR or immunocytochemistry.

Immunoblotting

Immunoblot analysis was performed as described (*48*) with some modifications. Blots were incubated with specific antibodies against Rho-kinase α (BD Biosciences Pharmingen) and MYPT (Santa Cruz Biotechnology). Rho-kinase activity was assessed by phosphorylation of MYPT and ERM with antibodies that specifically recognized MYPT phosphorylation at Thr^{696} (Upstate) (*49*) and ERM phosphorylation at ezrin (Thr^{567}), radixin (Thr^{564}), and moesin (Thr^{558}) (Cell Signaling Technology) (*50*).

RNA extraction and real-time PCR

Total RNA was extracted from mouse adipose tissue with the RNeasy lipid tissue kit (Qiagen). Total RNA was subjected to reverse transcription in a 20-μl reaction containing random primers and Superscript II enzyme (Invitrogen). Quantitative real-time PCR was performed with an ABI Prism 7700 Sequence Detection System using SYBR Green PCR Master Mix Reagent Kit (Applied Biosystems). Primers used are indicated in table S1. PCR-amplified products were also electrophoresed on agarose gels to confirm that single bands were amplified. mRNA expression was normalized to that of *GAPDH* (glyceraldehyde-3-phosphate dehydrogenase).

Statistical analysis

Data are expressed as means ± SEM. Data were analyzed by one- or two-way analysis of variance as appropriate, followed by Bonferroni's post hoc test. $P < 0.05$ was considered statistically significant.

SUPPLEMENTARY MATERIALS

www.sciencesignaling.org/cgi/content/full/4/157/ra3/DC1

Fig. S1. The effects of fasudil on adipocytokine mRNA in mature adipocytes.

Table S1. Primers used in real-time RT-PCR analysis.

REFERENCES AND NOTES

1. A. Lenz, F. B. Diamond Jr., Obesity: The hormonal milieu. *Curr. Opin. Endocrinol. Diabetes Obes.* **15**, 9–20 (2008).
2. N. Rasouli, P. A. Kern, Adipocytokines and the metabolic complications of obesity. *J. Clin. Endocrinol. Metab.* **93**, S64–S73 (2008).
3. F. Lago, C. Dieguez, J. Gómez-Reino, O. Gualillo, Adipokines as emerging mediators of immune response and inflammation. *Nat. Clin. Pract. Rheumatol.* **3**, 716–724 (2007).
4. G. S. Hotamisligil, Inflammation and metabolic disorders. *Nature* **444**, 860–867 (2006).
5. K. E. Wellen, G. S. Hotamisligil, Inflammation, stress, and diabetes. *J. Clin. Invest.* **115**, 1111–1119 (2005).
6. K. Kaibuchi, S. Kuroda, M. Amano, Regulation of the cytoskeleton and cell adhesion by the Rho family GTPases in mammalian cells. *Annu. Rev. Biochem.* **68**, 459–486 (1999).
7. K. Kimura, M. Ito, M. Amano, K. Chihara, Y. Fukata, M. Nakafuku, B. Yamamori, J. Feng, T. Nakano, K. Okawa, A. Iwamatsu, K. Kaibuchi, Regulation of myosin phosphatase by Rho and Rho-associated kinase (Rho-kinase). *Science* **273**, 245–248 (1996).
8. J. Pan, U. S. Singh, T. Takahashi, Y. Oka, A. Palm-Leis, B. S. Herbelin, K. M. Baker, PKC mediates cyclic stretch-induced cardiac hypertrophy through Rho family GTPases and mitogen-activated protein kinases in cardiomyocytes. *J. Cell. Physiol.* **202**, 536–553 (2005).
9. K. Numaguchi, S. Eguchi, T. Yamakawa, E. D. Motley, T. Inagami, Mechanotransduction of rat aortic vascular smooth muscle cells requires RhoA and intact actin filaments. *Circ. Res.* **85**, 5–11 (1999).
10. S. Kawamura, S. Miyamoto, J. H. Brown, Initiation and transduction of stretch-induced RhoA and Rac1 activation through caveolae: Cytoskeletal regulation of ERK translocation. *J. Biol. Chem.* **278**, 31111–31117 (2003).
11. T. Kanda, S. Wakino, K. Homma, K. Yoshioka, S. Tatematsu, K. Hasegawa, I. Takamatsu, N. Sugano, K. Hayashi, T. Saruta, Rho-kinase as a molecular target for insulin resistance and hypertension. *FASEB J.* **20**, 169–171 (2006).
12. Y. Nakayama, R. Komuro, A. Yamamoto, Y. Miyata, M. Tanaka, M. Matsuda, A. Fukuhara, I. Shimomura, RhoA induces expression of inflammatory cytokine in adipocytes. *Biochem. Biophys. Res. Commun.* **379**, 288–292 (2009).
13. Y. He, H. Xu, L. Liang, Z. Zhan, X. Yang, X. Yu, Y. Ye, L. Sun, Antiinflammatory effect of Rho-kinase blockade via inhibition of NF-κB activation in rheumatoid arthritis. *Arthritis Rheum.* **58**, 3366–3376 (2008).
14. N. Begum, O. A. Sandu, M. Ito, S. M. Lohmann, A. Smolenski, Active Rho-kinase (ROK-α) associates with insulin receptor substrate-1 and inhibits insulin signaling in vascular smooth muscle cells. *J. Biol. Chem.* **277**, 6214–6222 (2002).

15. C. Fischbach, T. Spruss, B. Weiser, M. Neubauer, C. Becker, M. Hacker, A. Göpferich, T. Blunk, Generation of mature fat pads in vitro and in vivo utilizing 3-D long-term culture of 3T3-L1 preadipocytes. *Exp. Cell Res.* **300**, 54–64 (2004).
16. M. Fasshauer, R. Paschke, Regulation of adipocytokines and insulin resistance. *Diabetologia* **46**, 1594–1603 (2003).
17. L. Makowski, J. B. Boord, K. Maeda, V. R. Babaev, K. T. Uysal, M. A. Morgan, R. A. Parker, J. Suttles, S. Fazio, G. S. Hotamisligil, M. F. Linton, Lack of macrophage fatty-acid–binding protein aP2 protects mice deficient in apolipoprotein E against atherosclerosis. *Nat. Med.* **7**, 699–705 (2001).
18. B. O. Shum, C. R. Mackay, C. Z. Gorgun, M. J. Frost, R. K. Kumar, G. S. Hotamisligil, M. S. Rolph, The adipocyte fatty acid–binding protein aP2 is required in allergic airway inflammation. *J. Clin. Invest.* **116**, 2183–2192 (2006).
19. A. Mishra, C. H. Cheng, W. C. Lee, L. L. Tsai, Proteomic changes in the hypothalamus and retroperitoneal fat from male F344 rats subjected to repeated light–dark shifts. *Proteomics* **9**, 4017–4028 (2009).
20. A. Rudich, H. Kanety, N. Bashan, Adipose stress-sensing kinases: Linking obesity to malfunction. *Trends Endocrinol. Metab.* **18**, 291–299 (2007).
21. S. L. Gray, A. J. Vidal-Puig, Adipose tissue expandability in the maintenance of metabolic homeostasis. *Nutr. Rev.* **65**, S7–S12 (2007).
22. G. Loirand, P. Guérin, P. Pacaud, Rho kinases in cardiovascular physiology and pathophysiology. *Circ. Res.* **98**, 322–334 (2006).
23. P. L. Rodriguez, S. Sahay, O. O. Olabisi, I. P. Whitehead, ROCK I-mediated activation of NF-κB by RhoB. *Cell. Signal.* **19**, 2361–2369 (2007).
24. Y. Funakoshi, T. Ichiki, H. Shimokawa, K. Egashira, K. Takeda, K. Kaibuchi, M. Takeya, T. Yoshimura, A. Takeshita, Rho-kinase mediates angiotensin II-induced monocyte chemoattractant protein-1 expression in rat vascular smooth muscle cells. *Hypertension* **38**, 100–104 (2001).
25. R. Sordella, W. Jiang, G. C. Chen, M. Curto, J. Settleman, Modulation of Rho GTPase signaling regulates a switch between adipogenesis and myogenesis. *Cell* **113**, 147–158 (2003).
26. M. Noguchi, K. Hosoda, J. Fujikura, M. Fujimoto, H. Iwakura, T. Tomita, T. Ishii, N. Arai, M. Hirata, K. Ebihara, H. Masuzaki, H. Itoh, S. Narumiya, K. Nakao, Genetic and pharmacological inhibition of Rho-associated kinase II enhances adipogenesis. *J. Biol. Chem.* **282**, 29574–29583 (2007).
27. S. Pellegrin, H. Mellor, Actin stress fibres. *J. Cell Sci.* **120**, 3491–3499 (2007).
28. R. P. Franke, M. Gräfe, H. Schnittler, D. Seiffge, C. Mittermayer, D. Drenckhahn, Induction of human vascular endothelial stress fibers by fluid shear stress. *Nature* **307**, 648–649 (1984).
29. B. Wojciak-Stothard, A. J. Ridley, Shear stress–induced endothelial cell polarization is mediated by Rho and Rac but not Cdc42 or PI 3-kinase. *J. Cell Biol.* **161**, 429–439 (2003).
30. D. P. Del Re, S. Miyamoto, J. H. Brown, Focal adhesion kinase as a RhoA-activable signaling scaffold mediating Akt activation and cardiomyocyte protection. *J. Biol. Chem.* **283**, 35622–35629 (2008).
31. N. Furukawa, P. Ongusaha, W. J. Jahng, K. Araki, C. S. Choi, H. J. Kim, Y. H. Lee, K. Kaibuchi, B. B. Kahn, H. Masuzaki, J. K. Kim, S. W. Lee, Y. B. Kim, Role of Rho-kinase in regulation of insulin action and glucose homeostasis. *Cell Metab.* **2**, 119–129 (2005).
32. D. H. Lee, J. Shi, N. H. Jeoung, M. S. Kim, J. M. Zabolotny, S. W. Lee, M. F. White, L. Wei, Y.-B. Kim, Targeted disruption of ROCK1 causes insulin resistance in vivo. *J. Biol. Chem.* **284**, 11776–11780 (2009).
33. J. P. Després, B. J. Arsenault, M. Côté, A. Cartier, I. Lemieux, Abdominal obesity: The cholesterol of the 21st century? *Can. J. Cardiol.* **24** (Suppl. D), 7D–12D (2008).
34. H. Kume, RhoA/Rho-kinase as a therapeutic target in asthma. *Curr. Med. Chem.* **15**, 2876–2885 (2008).
35. Y. He, H. Xu, L. Liang, Z. Zhan, X. Yang, X. Yu, Y. Ye, L. Sun, Antiinflammatory effect of Rho kinase blockade via inhibition of NF-κB activation in rheumatoid arthritis. *Arthritis Rheum.* **58**, 3366–3376 (2008).
36. M. Amano, H. Mukai, Y. Ono, K. Chihara, T. Matsui, Y. Hamajima, K. Okawa, A. Iwamatsu, K. Kaibuchi, Identification of a putative target for Rho as the serine-threonine kinase protein kinase N. *Science* **271**, 648–650 (1996).
37. S. R. Ross, R. A. Graves, A. Greenstein, K. A. Platt, H. L. Shyu, B. Mellovitz, B. M. Spiegelman, A fat-specific enhancer is the primary determinant of gene expression for adipocyte P2 in vivo. *Proc. Natl. Acad. Sci. U.S.A.* **87**, 9590–9594 (1990).
38. Y. Sasaki, M. Suzuki, H. Hidaka, The novel and specific Rho-kinase inhibitor (*S*)-(+)-2-methyl-1-[(4-methyl-5-isoquinoline)sulfonyl]-homopiperazine as a probing molecule for Rho-kinase-involved pathway. *Pharmacol. Ther.* **93**, 225–232 (2002).
39. S. Satoh, T. Utsunomiya, K. Tsurui, T. Kobayashi, I. Ikegaki, Y. Sasaki, T. Asano, Pharmacological profile of hydroxy fasudil as a selective rho kinase inhibitor on ischemic brain damage. *Life Sci.* **69**, 1441–1453 (2001).
40. S. Satoh, T. Yamaguchi, A. Hitomi, N. Sato, K. Shiraiwa, I. Ikegaki, T. Asano, H. Shimokawa, Fasudil attenuates interstitial fibrosis in rat kidneys with unilateral ureteral obstruction. *Eur. J. Pharmacol.* **455**, 169–174 (2002).
41. T. Jiang, Z. Wang, G. Proctor, S. Moskowitz, S. E. Liebman, T. Rogers, M. S. Lucia, J. Li, M. Levi, Diet-induced obesity in C57BL/6J mice causes increased renal lipid accumulation and glomerulosclerosis via a sterol regulatory element-binding protein-1c-dependent pathway. *J. Biol. Chem.* **280**, 32317–32325 (2005).
42. K. Kaku, F. T. Fiedorek Jr., M. Province, M. A. Permutt, Genetic analysis of glucose tolerance in inbred mouse strains. Evidence for polygenic control. *Diabetes* **37**, 707–713 (1988).
43. S. P. Weisberg, D. Hunter, R. Huber, J. Lemieux, S. Slaymaker, K. Vaddi, I. Charo, R. L. Leibel, A. W. Ferrante Jr., CCR2 modulates inflammatory and metabolic effects of high-fat feeding. *J. Clin. Invest.* **116**, 115–124 (2006).
44. W. Khazen, J. P. M'bika, C. Tomkiewicz, C. Benelli, C. Chany, A. Achour, C. Forest, Expression of macrophage-selective markers in human and rodent adipocytes. *FEBS Lett.* **579**, 5631–5634 (2005).
45. A. Masamune, K. Kikuta, M. Satoh, K. Satoh, T. Shimosegawa, Rho kinase inhibitors block activation of pancreatic stellate cells. *Br. J. Pharmacol.* **140**, 1292–1302 (2003).
46. C. X. Andersson, V. R. Sopasakis, E. Wallerstedt, U. Smith, Insulin antagonizes interleukin-6 signaling and is anti-inflammatory in 3T3-L1 adipocytes. *J. Biol. Chem.* **282**, 9430–9435 (2007).
47. Y. Tanabe, Y. Matsunaga, M. Saito, K. Nakayama, Involvement of cyclooxygenase-2 in synergistic effect of cyclic stretching and eicosapentaenoic acid on adipocyte differentiation. *J. Pharmacol. Sci.* **106**, 478–484 (2008).
48. S. Wakino, U. Kintscher, Z. Liu, S. Kim, F. Yin, M. Ohba, T. Kuroki, A. H. Schönthal, W. A. Hsueh, R. E. Law, Peroxisome proliferator-activated receptor γ ligands inhibit mitogenic induction of $p21^{Cip1}$ by modulating the protein kinase Cδ pathway in vascular smooth muscle cells. *J. Biol. Chem.* **276**, 47650–47657 (2001).
49. A. V. Somlyo, C. Phelps, C. Dipierro, M. Eto, P. Read, M. Barrett, J. J. Gibson, M. C. Burnitz, C. Myers, A. P. Somlyo, Rho-kinase and matrix metalloproteinase inhibitors cooperate to inhibit angiogenesis and growth of human prostate cancer xenotransplants. *FASEB J.* **17**, 223–234 (2003).
50. T. Matsui, M. Maeda, Y. Doi, S. Yonemura, M. Amano, K. Kaibuchi, S. Tsukita, S. Tsukita, Rho-kinase phosphorylates COOH-terminal threonines of ezrin/radixin/moesin (ERM) proteins and regulates their head-to-tail association. *J. Cell Biol.* **140**, 647–657 (1998).
51. **Acknowledgments:** We thank Y. Ogawa and T. Suganami from Tokyo Medical and Dental University for helpful discussions. We are also grateful to M. Amano from Nagoya University for providing information on the dominant-negative human RhoA construct. **Funding:** This work was supported by research funding from the Ministry of Education, Culture, Sports, Science and Technology, Japan. **Author contributions:** Y.H., S.W., H.T., S.T., and K.Y. did most of the experiments. Y.T. and M.S. did the cell stretch experiments. N.W., K. Homma, K. Hasegawa, H.M., K.F., and K. Hosoya did animal bleeding and assisted in the experiments. K.N. provided the stretch device. Y.H., S.W., K. Hayashi, and H.I. conceived and designed the project and wrote the manuscript. **Competing interests:** The authors declare that they have no competing interests.

Submitted 2 June 2010
Accepted 5 January 2011
Final Publication 25 January 2011
10.1126/scisignal.2001227
Citation: Y. Hara, S. Wakino, Y. Tanabe, M. Saito, H. Tokuyama, N. Washida, S. Tatematsu, K. Yoshioka, K. Homma, K. Hasegawa, H. Minakuchi, K. Fujimura, K. Hosoya, K. Hayashi, K. Nakayama, H. Itoh, Rho and Rho-kinase activity in adipocytes contributes to a vicious cycle in obesity that may involve mechanical stretch. *Sci. Signal.* **4**, ra3 (2011).

NDT Advance Access published March 4, 2011

Nephrol Dial Transplant (2011) 0: 1–10
doi: 10.1093/ndt/gfr012

Original Article

NDT
Nephrology Dialysis Transplantation

Rho-kinase inhibition ameliorates peritoneal fibrosis and angiogenesis in a rat model of peritoneal sclerosis

Naoki Washida[1], Shu Wakino[1], Yukio Tonozuka[2], Koichiro Homma[1], Hirobumi Tokuyama[1], Yoshikazu Hara[1], Kazuhiro Hasegawa[1], Hitoshi Minakuchi[1], Keiko Fujimura[1], Kohji Hosoya[1], Koichi Hayashi[1] and Hiroshi Itoh[1]

[1]Department of Internal Medicine, School of Medicine, Keio University, Tokyo, Japan and [2]Baxter Inc., Tokyo, Japan

Correspondence and offprint requests to: Shu Wakino; E-mail: swakino@sc.itc.keio.ac.jp

Abstract

Background. Peritoneal fibrosis (PF) and angiogenesis are typical morphological changes, leading to loss of peritoneal functions in patients undergoing peritoneal dialysis. The small G protein, Rho, and its downstream effector Rho-kinase have been shown to be involved in the tissue fibrosis process. This study was undertaken to investigate the role of Rho-kinase in the pathogenesis of these alterations.

Methods. PF was induced by intraperitoneal administration of chlorhexidine (CHX) in male rats (CHX group). These rats were treated with a Rho-kinase inhibitor, fasudil (Fas group). Human pleural mesothelial cells, MeT-5A cells, were stimulated by glucose with or without another Rho-kinase inhibitor, Y-27632.

Results. Peritoneal damage including peritoneal thickening, fibrous changes, macrophage migration and angiogenesis were evident in the CHX group and were ameliorated in the Fas group. The expression of markers of tissue fibrosis, such as transforming growth factor (TGF)-β, fibronectin and α-smooth muscle cell actin, were increased in the CHX group and were downregulated by fasudil. Similar results were also seen with an inducer of angiogenesis, vascular endothelial growth factor (VEGF). Rho-kinase was activated in the peritoneum of the CHX group, which was inhibited by fasudil. In MeT-5A cells, high glucose increased TGF-β expression and VEGF secretion, which were blocked by Y-27632.

Conclusions. The activation of Rho-kinase is involved in peritoneal damage at multiple stages including tissue fibrosis and angiogenesis. The inhibition of Rho-kinase constitutes a novel strategy for the treatment of PF.

Keywords: angiogenesis; peritoneal dialysis; peritoneal fibrosis; peritonium; Rho-kinase inhibitor

Introduction

Peritoneal dialysis (PD) is one treatment of choice of the treatments for end-stage renal failure. One of the long-term complications of PD is the decline of peritoneal function [1]. The decrease in ultrafiltration capacity after prolonged PD is an important reason for its discontinuation. Long-term PD is accompanied by functional and histopathological alterations in the peritoneum. Chronic peritoneal damage in PD is associated with multiple factors, including peritoneal fibrosis (PF), epithelial-messenchymal transition (EMT) of mesothelial cells and peritoneal neovascularization [2]. The pathogenesis of PF is a combination of bio-incompatible factors in the dialysate, including high glucose, high osmolality, advanced glycation products, glucose degradation products, uremic inflammation and acute peritonitis with inflammation [3]. A previous study demonstrated that glucose or glucose degradation products stimulate the production of transforming growth factor (TGF)-β, fibronectin and vascular endothelial growth factor (VEGF) from peritoneal mesothelial cells, which aggravated the progression of PF [4–7]. TGF-β has been reported to play a central role in tissue fibrosis, leading to a progressive loss of mesothelial cells [8]. Local production of VEGF plays a pivotal role in the angiogenesis of peritoneal tissues [9]. The expansion of the peritoneal vasculature is the main determinant of increased solute transport across the peritoneum that inhibits ultrafiltration capacity [10].

A serious complication of long-term PD is the development of encapsulating peritoneal sclerosis (EPS), which is characterized by bowel obstructions, various degrees of inflammation and enormous peritoneal thickening and encapsulation and cocooning [11]. It is also sometimes accompanied by peritoneal calcification [11]. These advanced lesions of PD complication need to be differentiated from PF and the final histological change of PF, peritoneal sclerosis (PS), as often seen in long-term PD patients without EPS [1]. Several factors were considered to be involved in the development of EPS, including PF, although the precise mechanisms have not yet been determined [12].

Small GTPase Rho-kinase, a member of the Rho-kinase subfamily of the Ras superfamily of monomeric GTPases, constitutes an important modulator of vascular smooth

muscle contraction [13]. Rho-kinase and its downstream effector Rho-kinase are important mediators not only of vascular contraction but also of actin cytoskeleton reorganization, cellular morphology, motility, adhesion and proliferation [14]. Because of its effects on various cellular functions, Rho-kinase has attracted significant interest as a potential target for the treatment of a wide range of pathological conditions including cancer, neuronal degeneration, kidney failure, asthma, glaucoma, osteoporosis, erectile dysfunction, insulin resistance and surgical adhesion. In practice, Rho-kinase inhibitor, fasudil, has already been in use for the prevention of vasospasm after the attack of subarachnoid hemorrhage [15]. One of the areas of interest has been their potential use for the prevention against the tissue fibrosis [16, 17].

Recent studies have witnessed that the Rho/Rho-kinase pathway is associated with tissue fibrosis and inflammation. It has also been demonstrated that the Rho/Rho-kinase pathway is involved in the tissue fibrosis process in various tissues through the regulation of TGF-β activation [18–20]. Y-27632, a specific Rho-kinase inhibitor, prevented the upregulation of α-smooth muscle actin (α-SMA), a marker of tissue fibrosis and inhibited tubulointerstitial fibrosis in mouse kidneys with unilateral ureteral obstruction [16]. In addition, the Rho/Rho-kinase pathway regulates hypoxia-induced VEGF expression [21]. These data in concert, suggested that Rho/Rho-kinase is involved in a final common pathway that aggravates the progression of peritoneal dysfunction.

Previously, we demonstrated that the Rho/Rho-kinase pathway is activated in the kidneys of subtotal nephrectomized rats, and the Rho-kinase inhibitor, fasudil, attenuated renal damage in the nephrectomized rats through amelioration of inflammatory changes of remnant kidneys [22]. In the present study, we investigated whether blocking of Rho-kinase similarly inhibited peritoneal damage by using both *in vivo* and *in vitro* systems. While a specific inhibitor, Y-27632 was administered in *in vitro* experiments to block Rho-kinase, we used fasudil in *in vivo* systems, although it is less specific for Rho-kinase. Fasudil is the Rho-kinase inhibitor practically available for long-term *in vivo* use. In addition, when it is administered *in vivo*, its metabolite, hydroxyfasudil, possesses a more selective action than its parent drug on Rho-kinase (specificity for Rho-kinase is 100 times higher for protein kinase C and 1000 times higher for myosin light chain kinase [23]). For these reasons, we selected fasudil to examine the effects of blocking Rho/Rho-kinase pathway *in vivo*. Our data demonstrated that Rho-kinase inhibitors ameliorated peritoneal damages and PF through direct effects on mesothelial cells.

Methods

Animals and peritoneal fibrosis model

Male Wistar rats (Saitama SLC, Saitama, Japan), weighing 150–200 g, were housed in a controlled environment, fed a standard rat chow (0.19% sodium, 0.74% potassium and 20.6% protein; Oriental Yeast Co., Itabashi, Tokyo) and allowed free access to water. Peritoneal inflammation and a sclerosis model was made by injection of a chlorhexidine (CHX) solution consisting of 0.1% CHX gluconate and 15% ethanol intraperitoneally for 4 weeks to male Wister rats at the age of 6 weeks [22, 23]. The rats were fed a standard laboratory diet and allowed free access to water. The rats were treated daily with CHX solution into the peritoneal cavity. The animals were sacrificed 4 weeks after the first CHX solution injection and the peritoneal tissues were dissected carefully for further analysis. All experiments were performed in accordance with the animal experimentation guideline of Keio University School of Medicine.

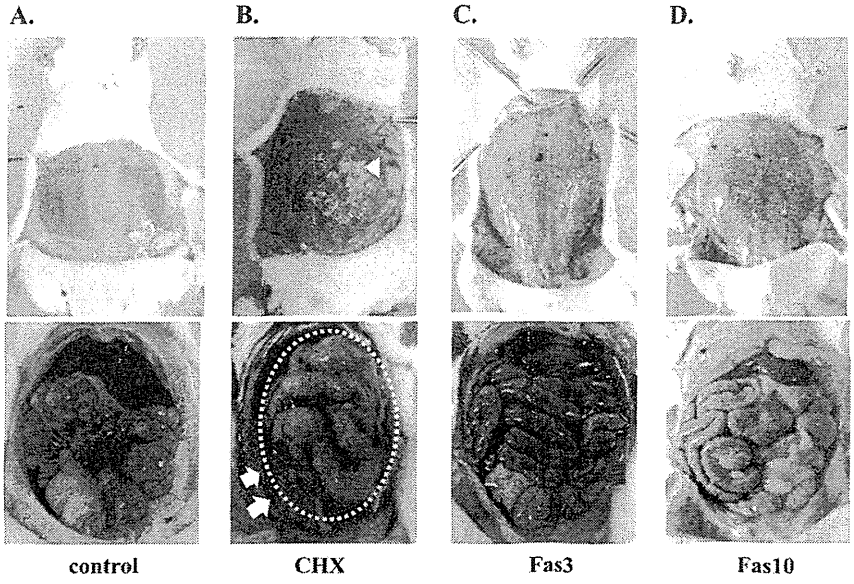

Fig. 1. The effects of the Rho-kinase inhibitor, fasudil, on the macroscopic findings of CHX-induced peritoneal damage. PF was induced in male Wister rats with an intraperitoneal injection of CHX for 4 weeks (**B**). Control rats were subjected to saline injection (**A**). Severe inflammatory changes of peritonium was evident and presented with bowel dilatation, calcification (white triangles), ascites with bleeding (white arrows) and cocoon formation (dotted lined circle). Treatment with fasudil at dosages of 3 mg/kg (Fas3; **C**) and 10 mg/kg (Fas10; **D**) ameliorated these peritoneal damages. Each photograph showed the representative peritoneum (upper panel) and bowel (lower panel) finding in each group.

Animal study protocol

Rats were assigned to four groups: Group 1, rats injected with 2 mL of normal saline (control group, $n = 6$); Group 2, rats injected intraperitoneally with CHX solution (CHX group, $n = 6$); Group 3, rats injected intraperitoneally with CHX solution and 3 mg/kg/day Rho-kinase inhibitor, fasudil (Asahi Kasei, Tokyo, Japan) (Fas3 group, $n = 6$) and Group 4, rats injected intraperitoneally with CHX solution and 10 mg/kg/day fasudil (Fas10 group, $n = 6$). The dosage of fasudil was determined in agreement with previous reports [20, 21].

Histological examination and immunohistochemistry

At sacrifice, intraperitoneal macroscopic views were compared among the four groups. We defined the rats with EPS-like changes as those showing three of five findings: peritoneal calcification, bowel dilatation, bowel adhesion, ascites with bleeding and cocoon formation. We counted the affected rats in each group ($n = 6$), although the extent of peritoneal changes in each rat were different in each group. Three pieces of the mid-parietal peritoneal membrane adjacent to the rectus abdominal muscle were excised. One of these pieces was fixed in 10% buffered formaldehyde, embedded in paraffin and stained with Masson's trichrome solution. Submesothelial thickening was identified as the membrane area extending from the surface mesothelium to the upper limit of the muscular tissues. We measured peritoneal thickness at six random points. Quantification of fibrous tissue area was performed by measuring the Masson's trichrome-stained area at 20 consecutive fields of peritoneal tissues of each group. The number of vessels in the submesothelial zone outside the muscle layer was counted in 10 fields of peritoneal tissues of each group. Fibrous tissue area, peritoneal thickness and the number of vessels were evaluated by Win Roof ver. 6.0 software (Mitani Corp., Tokyo, Japan). These analyses were performed on an individual rat by two investigators in a blinded fashion. Other pieces were embedded in paraffin and used for immunostaining using antibodies against CD68 (AbDserotec, Oxford, UK) and α-SMA (Dako Cytomation, Glostrup, Denmark). Cells stained with α-SMA were counted by computer-aided planimetry using the Scion Image software.

Cell culture and experimental protocols

The human pleural mesothelial cell line MeT-5A was purchased from American Type Culture Collection (Rockville, MD) and cultured in Dulbecco's modified Eagle's medium Nutrient Mixture F-12 (GIBCO) with 10% fetal calf serum, penicillin and streptomycin in a humidified 5% CO2 incubator at 37°C [23, 25]. Although this cell line is derived from pleural tissues, it was utilized because its response to the cellular external stress was demonstrated to be similar to primary peritoneal mesothelial cells [26, 27] and because it showed high viability and good biological response to glucose stimulation. The cells were seeded at a density of 1×10^5 cells per well on a 48-well plate. After MeT-5A cells were grown to 60–70% confluence and made quiescent by serum starvation (0.4%, fetal bovine serum) and normal glucose conditions (5 mmol/L) for 24 h, Rho-kinase inhibitor, Y-27632, was added at three different concentrations of 1, 5 and 10 μmol/L. Thirty minutes after treatment with Y-27632, cells were stimulated with a high concentration of glucose (200 mmol/L) [28]. Eight hours after stimulation, cell lysates were obtained for further analysis [29]. Cell

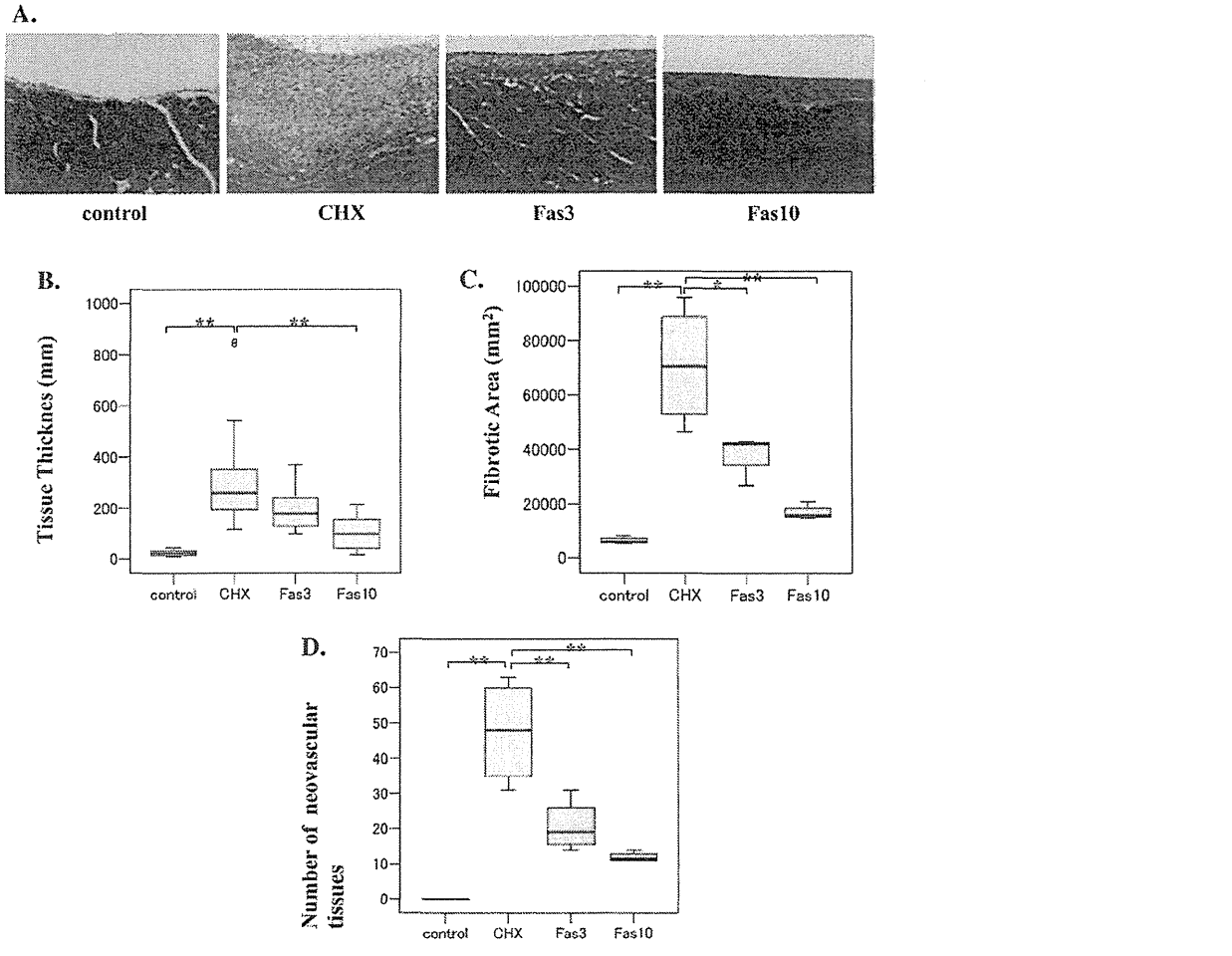

Fig. 2. The effects of fasudil on the histological changes of CHX-induced peritoneal damage. (**A**) Histological findings of the anterior abdominal wall stained with Masson's trichrome solution. Thickness of the peritoneum (**B**), area of fibrous tissues (**C**) and the number of neovascular tissues (**D**) were analyzed in control rats (control), rats with CHX-induced peritoneal damage (CHX) and rats with peritoneal damage treated with 3 mg/kg (Fas3) and 10 mg/kg (Fas10) of fasudil. **P < 0.01 versus CHX group, *P < 0.05 versus CHX group, $n = 6$.

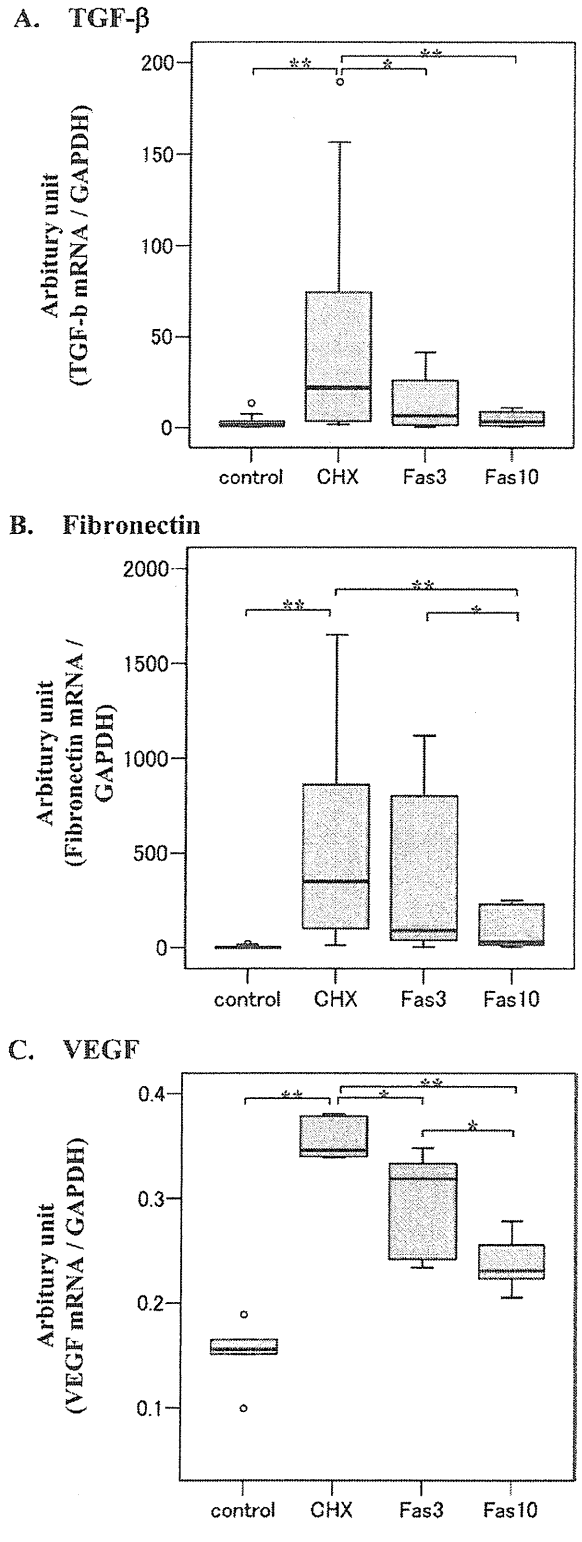

Fig. 3. The effects of fasudil on the mRNA expressions of TGF-β, fibronectin and VEGF in peritoneal tissues. The mRNA expression of TGF-β (**A**), fibronectin (**B**) and VEGF (**C**) in the peritoneal tissues were measured by real-time PCR as described in the Methods section in control rats (control), rats with CHX-induced peritoneal damage (CHX) and rats with peritoneal damage treated with 3 mg/kg (Fas3) and 10 mg/kg (Fas10) of fasudil. **P < 0.01 versus CHX group, *P < 0.05 versus CHX group, $n = 6$.

culture supernatants were also obtained 24 h after stimulation to measure the concentration of VEGF with the quantitative sandwich enzyme immunoassay technique (Quantikine; R&D Systems).

RNA extraction and real-time polymerase chain reaction

Total RNA was extracted from the rat mid-parietal peritoneal tissues with the adjacent muscle tissues using TRIzol reagent [28]. Equal amounts (2 μg) of total RNA from each sample were converted to complementary DNA by M-MLV reverse transcriptase RNaseH with oligo dT20 primer (Invitrogen, Carlsbad, CA) in a 20 μL reaction volume. Real-time polymerase chain reaction (PCR) was performed using LightCycler quick systems 350S (Roche Diagnostics, Tokyo, Japan). Amplification products were analyzed by a melting curve, which confirmed the presence of a single PCR product in all reactions. Levels of messenger RNA (mRNA) were normalized to those of glyceraldehyde 3-phosphate dehydrogenase (GAPDH). The primer sequences were as follows: TGF-β1, sense 5′-AGAAGTCACCCG-CGTGCTAA-3′ and antisense 5′-TCCCGAATGTCTGACGTATTGA-3′; fibronectin, sense 5′-GTGTCTCCAGCGTGTACGAA-3′ and antisense 5′-GGCGGTGACATCAGAAGAAT-3′; VEGF, sense 5′-CATGC-CAAGTGGTCCCA-3′ and antisense 5′-CTATCTTTCTTTGGTCTG-CATTCAC-3′; α-SMA, sense 5′-TGCTGGACTCTGGAGATG-3′ and antisense 5′-GTGATCACCTGCCCATC-3′; GAPDH, sense 5′-CCTGCCAAGTATGATGACATCAAGA-3′ and antisense 5′-GTAGCC-CAGGATGCCCTTTAGT-3′. The amplification program was 95°C for 3 min and then 40 cycles consisting of 95°C for 10 s, 62°C for 10 s and 72°C for 10 s.

Immunoblotting analysis to evaluate the activity of Rho-kinase was performed as described previously [28] by using rat mid-parietal peritoneal tissues with the adjacent muscle tissues. Peritoneal tissues were lysed in 500 μL of ice-cold lysis buffer and centrifuged at 15 000 *g* for 20 min. Supernatant aliquots were subject to immunoblotting using primary antibody against phosphorylated myosin phosphatase target subunit (MYPT1), Rho-kinase substrate (Millipore, Billerica, MA). After the incubation with primary antibody blots were incubated with secondary antibody (horseradish peroxidase-conjugated donkey anti-rabbit IgG; Millipore). Immunoreactive bands were detected using an ECL detection kit (Millipore). Band intensity was determined by using NIH image software (version 1.6).

Data analysis

Statistical analysis was performed using the SPSS 12 software package (SPSS, Chicago, IL). Results are expressed as mean ± SEM of at least three individual experiments. Statistical analysis was performed with analysis of variance followed by Tukey's post-hoc test unless otherwise stated. Differences with $P < 0.05$ were considered statistically significant.

Results

Effects of fasudil on the macroscopic view of peritoneal fibrosis

Four-week intraperitoneal administration with CHX solution induced PS with bowel dilatation, bowel adhesion, peritoneal calcification (Figure 1B, white triangle), ascites with bleeding (Figure 1B, white arrows) and cocoon formation (Figure 1B, dotted lined circle). These findings were similar to those in the patients with EPS (Figure 1). Five of six rats (83.3%) in the CHX group had peritoneal damage which was defined as the rats showing three of five peritoneal and bowel findings as described above. These changes were attenuated by treatment with fasudil in a dose-dependent manner. Thus, two of six rats were affected by the treatment with 3 mg/kg fasudil (Fas3; 33.3%) and none of the six rats by the treatment with 10 mg/kg fasudil (Fas10).

Effects of fasudil on the peritoneal histological changes

After 4-week administration of CHX, peritoneal samples showed markedly increased peritoneal thickness with

mean thickness of 307.6 ± 123.7 μm as compared to that of control rats (22.9 ± 6.7 μm) (Figure 2B, $P < 0.001$, $n = 6$). Treatment with fasudil ameliorated these changes in a dose-dependent manner (Figure 2B, Fas3 group: 185.2 ± 67.1 μm; Fas10 group: 111.5 ± 48.1 μm; $P < 0.001$ versus CHX group, $n = 6$). Masson's trichrome staining revealed that the fibrous area in the submesothelial compact zone of the rats' peritoneum in the CHX group was significantly increased as compared to that of control rats (Figure 2C, control versus CHX: 5815.2 ± 1551.9 μm^2 versus 62 462.3 ± 21 941.2 μm^2, $P < 0.001$, $n = 6$). These increases of tissue fibrotic changes were ameliorated by the treatment with fasudil in a dose-dependent manner (Figure 2C, Fas3 group: 35 666.2 ± 9188.5 μm^2, $P < 0.01$ versus CHX group, $n = 6$; Fas10 group: 16 859.0 ± 2698.7 μm^2, $P < 0.001$ versus CHX group, $n = 6$). Neovascularization of the peritoneum is also characteristic of CHX-induced peritoneal fibrosis as well as peritoneal damage observed in long-term PD patients. The number of vessels, determined by immunostaining with CD31, in the peritoneum of CHX-group rats was increased compared to that of control rats (Figure 2D, control versus CHX: 0.2 ± 0.4/high power field (HPF) versus 43.5 ± 13.3/HPF, $P < 0.001$, $n = 6$ for each group), which was also attenuated by treatment with fasudil in a dose-dependent manner (Figure 2D, Fas3 group: 20.0 ± 6.6/HPF, $P < 0.001$ versus CHX group, $n = 6$ for each group, Fas10 group: 12.0 ± 1.4/HPF, $P < 0.001$ versus CHX group, $n = 6$ for each group).

Effects of fasudil on the expressions of TGF-β, fibronectin and VEGF in peritoneal tissues

The molecular mechanism(s) for the histological improvement by fasudil was investigated by examining the expression of TGF-β and VEGF, humoral mediators for fibrosis and neovascularization, respectively. The mRNA level of TGF-

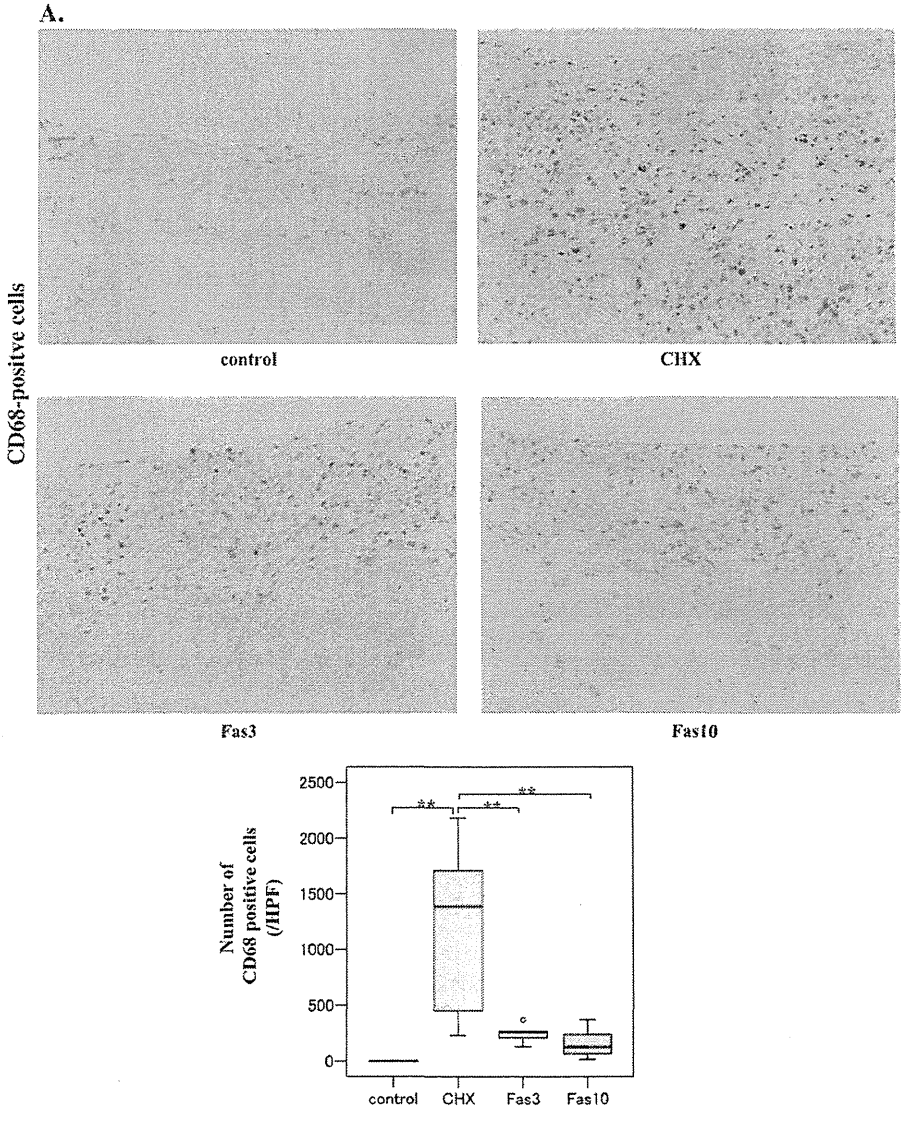

Fig. 4. Continued on following page

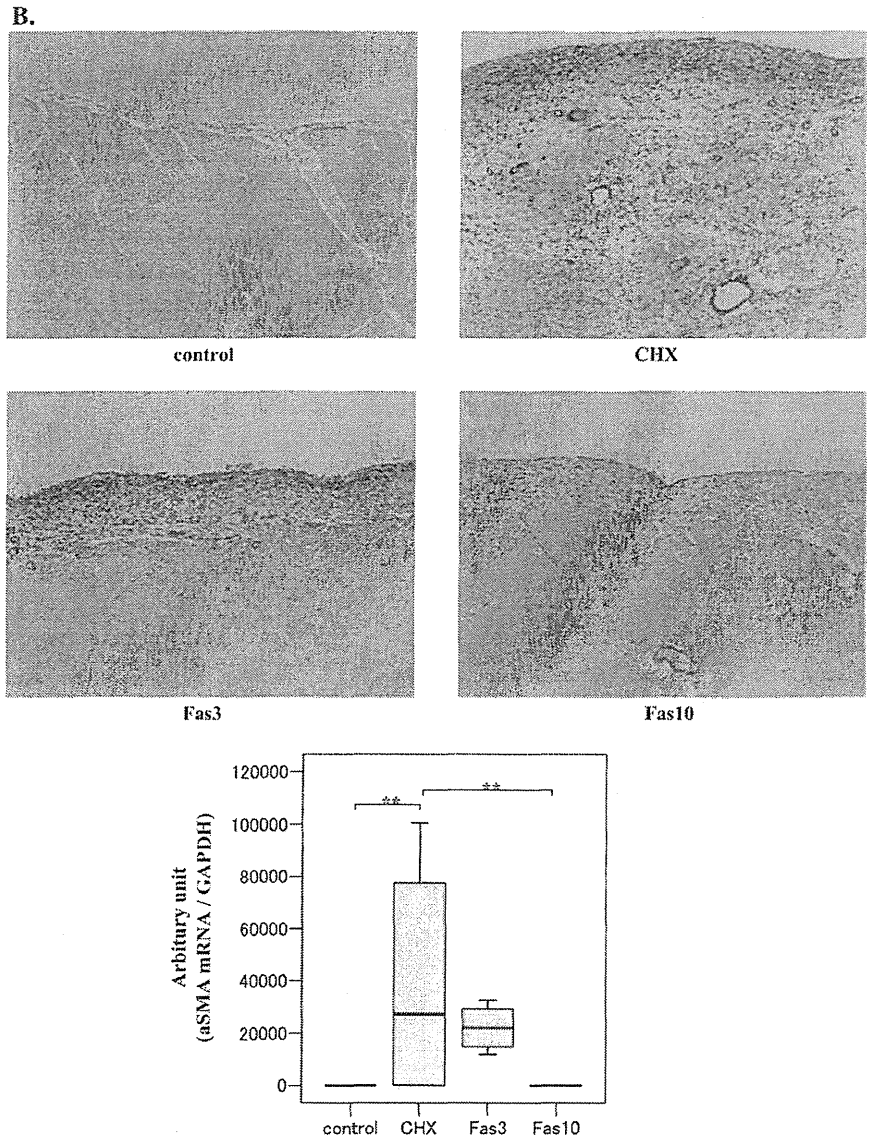

Fig. 4. The effects of fasudil on inflammatory and fibrotic changes in CHX-damaged peritoneal tissues. (**A**) Immunohistochemical analysis by CD68 staining is shown in the upper panel. The number of CD68-positive macrophages were quantified and compared among the control rats (control), rats with CHX-induced peritoneal damage (CHX) and rats with peritoneal damage treated with 3 mg/kg (Fas3) and 10 mg/kg (Fas10) of fasudil (lower panel). **P < 0.01 versus CHX group, *P < 0.05 versus CHX group, $n = 6$. (**B**) Immunohistochemical analysis by α-SMA staining is shown in the upper panel. The mRNA expression of α-SMA was quantified by real-time PCR among control rats (control), rats with CHX-induced peritoneal damage (CHX) and rats with peritoneal damage treated with 3 mg/kg (Fas3) and 10 mg/kg (Fas10) of fasudil (lower panel). **P < 0.01 versus CHX group, *P < 0.05 versus CHX group, $n = 6$.

β was increased in the peritoneum of rats in the CHX group 10.3-fold, which was attenuated by treatment with fasudil in a dose-dependent manner (Figure 3A, Fas3 group: 62.2% inhibition, P < 0.05 versus CHX group, $n = 6$; Fas10 group: 84.2% inhibition, P < 0.01 versus CHX group, $n = 6$). Consistently, mRNA expression of fibronectin, a marker of tissue fibrotic changes, of rats in the CHX group was upregulated 75.4-fold as compared with that in the control group (P < 0.01, $n = 6$). Treatment with fasudil attenuated the increased expression of fibronectin in a dose-dependent manner (Figure 3B, Fas3 group: 20.9% inhibition, P < 0.05 versus CHX group, $n = 6$; Fas10 group: 80.0% inhibition, P < 0.01 versus CHX group, $n = 6$). Similarly, mRNA expression of VEGF was increased in the peritoneum of rats in the CHX group 2.1-fold, which was attenuated by treatment with fasudil in a dose-dependent manner (Figure 3C, Fas3 group: 18.1% inhibition, P < 0.05 versus CHX group, $n = 6$; Fas10 group: 34.9% inhibition, P < 0.01 versus CHX group, $n = 6$).

Effects of fasudil on inflammatory changes and EMT in the CHX-damaged peritoneal tissues

Fibrotic changes of the peritoneum are preceded partly by inflammation of the peritoneum. To assess inflammatory

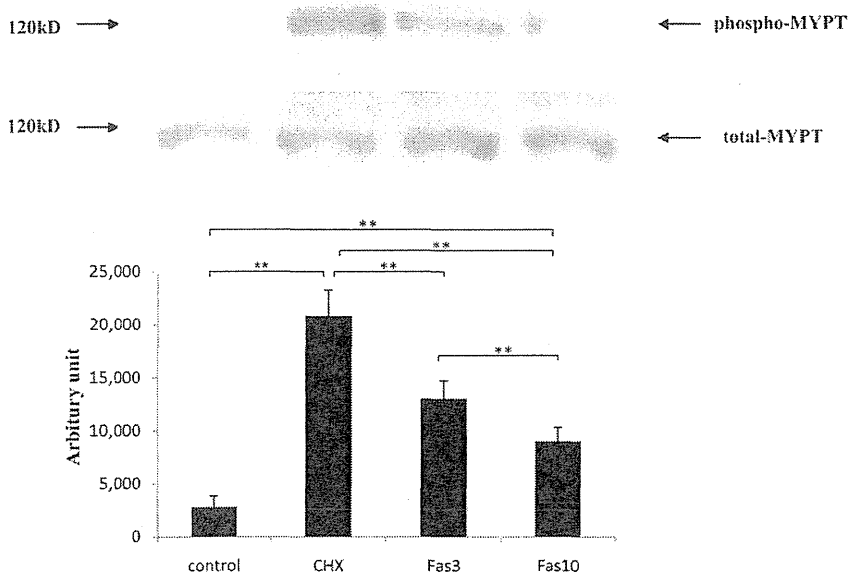

Fig. 5. Rho-kinase activity in the peritoneal tissues. The activity of Rho-kinase was evaluated by immunoblotting using antibody against phosphorylated MYPT, a substrate of Rho-kinase in control rats (control), rats with CHX-induced peritoneal damage (CHX) and rats with peritoneal damage treated with 3 mg/kg (Fas3) and 10 mg/kg (Fas10) of fasudil (upper panel). Immunoblots for total MYPT were loading controls (upper panel). Densitometric analysis was shown in the lower panel. **P < 0.01 between the two group, $n = 6$. The blots shown here were representative of three independent experiments.

changes, invasion of macrophages in the peritoneum was examined by immunostaining with CD68, a cell surface marker of macrophages. As shown in Figure 4A, the staining with CD68 was enhanced in the peritoneum of rats in the CHX group, which was significantly attenuated by treatment with fasudil in a dose-dependent manner (Fas3: 79.2% inhibition, P < 0.01, $n = 6$; Fas10: 88.4% inhibition, P < 0.01, $n = 6$). Immunostaining for α-SMA, one of the markers of fibrosis in the tissues was also examined. Staining was increased in the CHX group compared to the control group, which was also attenuated by treatment with fasudil in a dose-dependent manner (Fas3: 48.5 % inhibition, P = 0.51, $n = 6$; Fas10: 99.9% inhibition, P < 0.01, $n = 6$, Figure 4B, upper panel). Consistently, mRNA expression of α-SMA in the peritoneum of rats in the CHX group was enhanced in comparison with that in control rats (P < 0.01, $n = 6$, Figure 4B, lower panel), which was significantly attenuated by treatment with fasudil (Fas3: 46.7% inhibition, P = 0.54, $n = 6$; Fas10: 99.9% inhibition, P < 0.01, $n = 6$, Figure 4B, lower panel).

Rho-kinase activity in the peritoneal tissues

In order to explore the role of Rho-kinase in the pathogenesis of CHX-induced peritoneal fibrosis, the activity of Rho-kinase was evaluated by immunoblotting using an antibody against phosphorylated MYPT, a substrate of Rho-kinase. Rho-kinase activity in the peritoneum of rats in the CHX group was enhanced when compared with that of control rats (Figure 5, 3.5-fold induction versus control group, P < 0.01, $n = 6$). The activation of Rho-kinase was inhibited by treatment with fasudil (Figure 5, Fas3 group: 43.6% inhibition, P < 0.01 versus CHX group, $n = 6$; Fas10 group: 74.3% inhibition, P < 0.01 versus CHX group, $n = 6$). These data indicated that Rho/Rho-kinase pathway was activated in CHX-induced peritoneal damage, which was successfully inhibited by the treatment with fasudil.

Effects of Y-27632 on TGF-β expression and VEGF production in MeT-5A cells

To examine whether the effects of Rho-kinase inhibition was its direct action on mesothelial cells, an *in vitro* study utilizing the mesothelial cell line, MeT-5A cells, was performed. Stimulation of MeT-5A cells with high glucose (200 mmol/L) upregulated mRNA expression of TGF-β 10.5-fold as compared with that of quiescent cells (P < 0.01), which was inhibited by pretreatment with the Rho-kinase inhibitor, Y-27632, in a dose-dependent manner (Figure 6A, 5 μmol/L, Y5: 69.3% inhibition, P < 0.05 $n = 5$; 10 μmol/L, Y10: 81.5% inhibition, P < 0.01 versus glucose-stimulated cells, $n = 5$). Secretion of VEGF in the medium was increased in glucose-stimulated MeT-5A cells (3.0-fold induction, P < 0.05 versus quiescent cells, $n = 5$), which was also inhibited by Y-27632 in a dose-dependent manner (Figure 6B, 5 μmol/L, Y5: 14.7% inhibition, P < 0.05 $n = 5$; 10 μmol/L, Y10: 25.2% inhibition, P < 0.05 versus glucose-stimulated cells, $n = 5$). These data implied that the effects of Rho-kinase inhibition were partly due to direct action on mesothelial cells.

Discussion

During long-term PD, morphological and functional changes of the peritoneal membrane lead to ultrafiltration failure and inefficient elimination of solutes. Typical

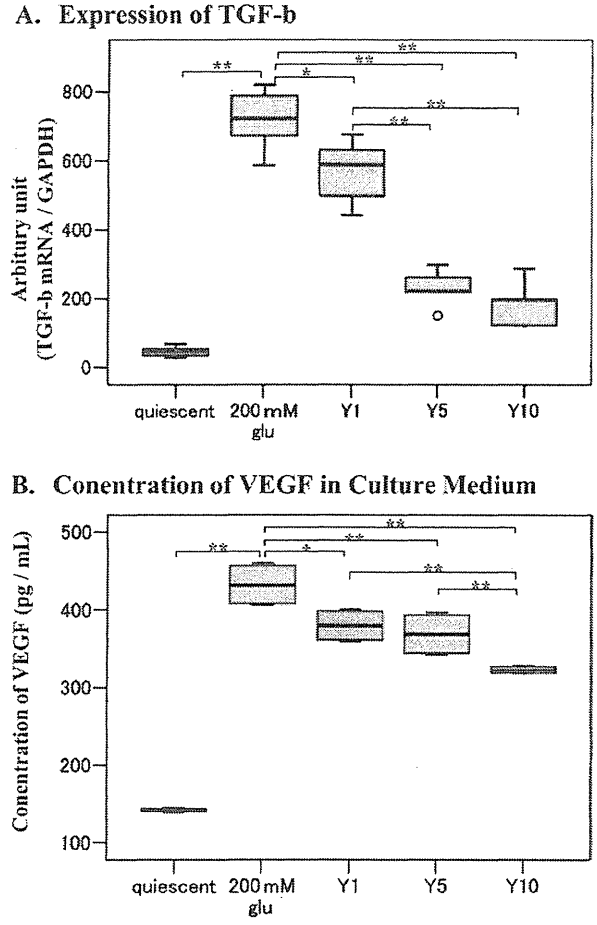

Fig. 6. Effects of Y-27632 on TGF-β expression and VEGF production in MeT-5A cells. Serum-starved mesothelial cells (quiescent) were stimulated with high glucose (200 mmol/L glucose) in the presence or absence of Rho-kinase inhibitor, Y-27632 at concentrations of 1 μmol/L (Y1), 5 μmol/L (Y5) and 10 μmol/L (Y10). The mRNA expression of TGF-β in the cell (upper panel) and the concentration of VEGF in the medium (lower panel) were analyzed by real-time PCR and enzyme-linked immunosorbent assay, respectively. $^{**}P < 0.01$ versus CHX group, $^{*}P < 0.05$ versus CHX group, $n = 5$.

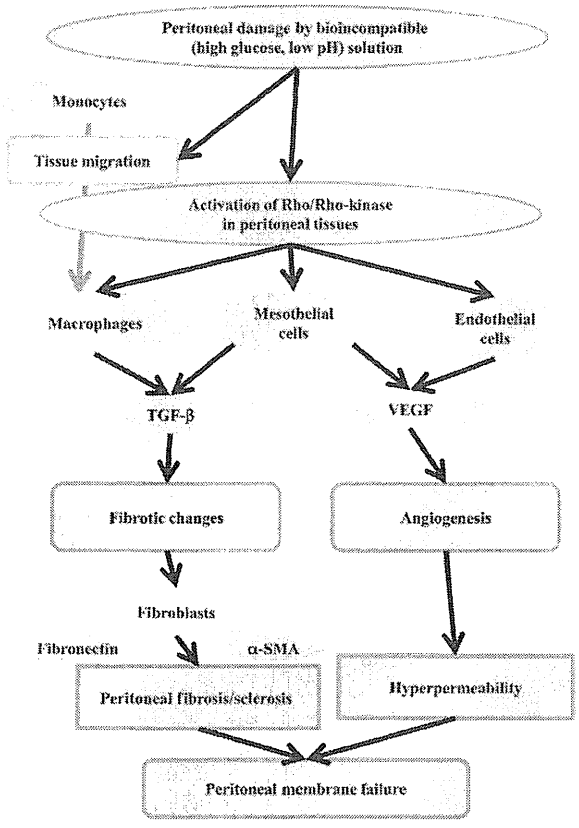

Fig. 7. Schema depicting the molecular mechanism for peritoneal damage through the activation of Rho/Rho-kinase pathway. Peritoneal tissue damage is induced by bioincompatible dialysis solution, which provoked migration of inflammatory cells and activation of the Rho/Rho-kinase pathway in each cell type present in the peritoneal tissues, monocytes/macrophages, mesothelial cells and endothelial cells. Activation of the Rho/Rho-kinase pathway in the peritoneal tissues induced tissue fibrosis and angiogenesis through the increased expression of TGF-β and VEGF, respectively. Angiogenesis leads to hyperpermeable peritoneal tissues. Both fibrosis and angiogenesis deteriorate peritoneal membrane function and result in ultrafiltration failure or increased transport of small solutes. Blocking this pathway halts these tissue alterations and prevents peritoneal membrane failure.

morphological alterations of the peritoneal membrane are submesothelial fibrosis, angiogenesis and inflammatory cell infiltration [29]. These peritoneal changes of PF and PS result in a serious clinical complication, EPS, although other factors than PS were involved in its pathogenesis (Figure 7). In the present study, we utilized a rat model with CHX-induced PF, which has been reported to mimic the peritoneal pathological changes in long-term PD patients, such as the pathological changes observed in PS and EPS [30, 31]. We demonstrated that the Rho-kinase inhibitor, fasudil successfully prevented the progression of PS. In addition, as shown in the present study (Figure 1), this model has a macroscopic appearance of EPS in the peritoneum and small intestine. Using this model, several reagents have been tested as therapeutic strategies against PS, including rennin–angiotensin system blockade [32], erythropoietin [24] and antifibrotic agent, pirfenidone [33]. In this study, we demonstrated that administration of fasudil inhibited the peritoneal fibrotic changes and blocked progression to EPS, which can constitute a novel therapeutic strategy for the prevention of EPS in long-term PD patients.

One of the first steps of PF is inflammatory damage to the mesothelial tissues, which is initiated by the recruitment of inflammatory cells. Another mechanism is that glucose degradation products, directly through the action receptor for advanced glycation end-products, could upregulate TGF-β and cause fibrosis. The damage of peritoneal mesothelial cells cause the peritoneal adhesion and dysfunction. Histological findings of damaged peritoneum in our rat models revealed that macrophages (CD68-positive cells) migrating from vascular tissues move on the surface of the peritoneum and reside in a line (Figure 4A). Studies in vascular tissues have suggested that monocyte recruitment into the vessel wall is usually promoted by chemokines, such as monocyte chemoattractant protein-1, which is an early step in the process of arteriosclerosis [13]. Rho-kinase is involved in macrophage-mediated

formation of coronary vascular lesions in an *in vivo* porcine model and a Rho-kinase inhibitor, hydroxyl-fasudil markedly inhibited macrophage accumulation and migration [34]. In this study, as a result of the inhibitory effects of fasudil on macrophage migration, the initiation of peritoneal tissue inflammation was attenuated and the expressions of fibrotic factor, TGF-β, fibronectin and various inflammatory cytokines which, in part, were secreted by migrated inflammatory cells, were downregulated. These effects contributed to blocking the aggravation of peritoneal damages.

Various humoral factors from migrated macrophages or mesothelial cells were suggested to be involved in the development of PS. Among them, TGF-β plays the most essential role in the initiation of PS by EMT of peritoneal mesothelial cells [35, 36]. Consistently, blockade of TGF-β has been shown to prevent the development of PF in rat PF models [8]. Accumulating evidence has been reported that the Rho/Rho-kinase pathway participates importantly in the process of tissue fibrosis as well as EMT in several tissue culture systems [37–41]. We previously reported that Rho-kinase inhibitor attenuates renal inflammatory changes in remnant kidney models and that, through its inhibitory effects on the Rho/Rho-kinase pathway, the T-type calcium channel blocker attenuated renal fibrotic changes of the rat model [42]. In the present study, the Rho-kinase inhibitor downregulated the increased expression of TGF-β and fibronectin in the peritoneal membrane of rats with CHX-induced PF. Furthermore, fasudil markedly inhibited the expression of α-SMA mRNA and decreased α-SMA immunostaining, which suggested its inhibitory effects on the fibrotic changes by mesothelial cells. Finally, Masson's trichrome staining revealed that the Rho-kinase inhibitor reduced thickening of the peritoneal membrane and decreased the fibrotic component. The present study provides a novel therapeutic strategy for prevention against the initiation and the progression of PF and its serious complication, EPS. The mechanisms involved in this PF were summarized in Figure 7.

Besides inflammation and fibrosis, an increased number of capillaries are also related to peritoneal membrane failure [1, 43]. Angiogenesis is involved in elevation of small-solute transport across the peritoneal membrane and in ultrafiltration failure. Peritoneal expression of VEGF is correlated with the degree of angiogenesis [44]. Our rat models of peritoneal damage presented with the increased number of capillaries and the increased expression of VEGF in the peritoneal membrane, which were attenuated by treatment with fasudil. Y-27632 inhibited secretion of VEGF from MeT-5A cells, although the expression levels in the cells were not altered (data not shown). Therefore, inhibitory effects by fasudil resulted from its effects on endothelial cells or on transdifferentiated mesothelial cells because transformed not intact mesothelial cells are an important source of VEGF in PD patients [45]. The expression of VEGF was regulated by the Rho/Rho-kinase pathway in vascular endothelial cells [46]. Our *in vitro* data indicated that, in addition to endothelial cells, peritoneal mesothelial cells also produced VEGF, which might contribute to angiogenesis in the submesothelial cell layer in the peritoneum and to the regulation of peritoneal permeability. Y-27632 blocked secretion of VEGF from MeT-5A cells, which underscored activation of the Rho/Rho-kinase pathway as a potential mechanism for angiogenesis in the damaged peritoneum. Bleeding through the neovascular tissues created an accumulated fibrin layer and resulted in the cocoon formation. As evident in the improvement in macroscopic findings of peritoneum in rats treated with fasudil, inhibition by Rho-kinase prevented bleeding and further damage to peritoneal tissues. These mechanisms involved in angiogenesis were summarized in Figure 7.

In the present study, peritoneal sclerosing models were made by injection of CHX solution intraperitoneally. This model does not precisely reflect the pathology of EPS and PS in PD patients. We were also unable to consider the extent to which uremia affected peritoneal membrane damages. Moreover, we observed that since peritoneal damages were induced by the intraperitoneal injection of CHX in this model, the affected lesion appeared to be widely dispersed, which caused the values of CHX group with wide variances. However, several studies already have shown similarities of pathological changes in peritoneal tissues between this models and long-term PD patients [24, 30, 31]. In addition, in an *in vitro* study, we utilized MeT-5A cell line whose phenotype is not completely similar to that of peritoneal mesothelial cells [26]. In spite of these limitations, this study demonstrated that the Rho-kinase inhibitor ameliorated the development of peritoneal damage. Since no promising therapeutics have been established for peritoneal injury in PD patients, the Rho-kinase inhibitor may be a novel strategy as a protective agent for peritoneal damages and the ensuing PS.

Acknowledgements. This research was supported by Baxter dialysis fund.
Transparency declarations. Y.T. is an employee of Baxter Inc., Japan.

Conflict of interest statement. None declared.

References

1. Margetts PJ, Bonniaud P. Basic mechanisms and clinical implications of peritoneal fibrosis—in depth review. *Perit Dial Int* 2003; 23: 530–541
2. Margetts PJ, Kolb M, Galt T *et al.* Gene transfer of transsorming growth factor-beta1 to the rat peritoneum: effects on membrane function. *J Am Soc Nephrol* 2001; 12: 2029–2039
3. Krediet RT, Lindholm B, Rippe B. Pathophysiology of peritoneal membrane failure. *Perit Dial Int* 2000; 20: S222–S242
4. Leung JC, Chan LY, Tam KY *et al.* Regulation of CCN2/CTGF and related cytokines in cultured peritoneal cells under conditions simulating peritoneal dialysis. *Nephrol Dial Transplant* 2009; 24: 458–469
5. Xu ZG, Kim KS, Park HC *et al.* High glucose activates the p38 MAPK pathway in cultured human peritoneal mesothelial cells. *Kidney Int* 2003; 63: 958–968
6. Mandl-Weber S, Cohen CD, Haslinger B *et al.* Vascular endothelial growth factor production and regulation in human peritoneal mesothelial cells. *Kidney Int* 2002; 61: 570–578
7. Witowski J, Korybalska K, Ksiazek K *et al.* Peritoneal dialysis with solutions low in glucose degradation products is associated with improved biocompatibility profile towards peritoneal mesothelial cells. *Nephrol Dial Transplant* 2004; 19: 917–924
8. Liu Y. Epithelial to messenchymal transition in renal fibrogenesis; Pathologic significance, molecular mechanism, and therapeutic intervention. *J Am Soc Nephrol* 2004; 15: 1–12

9. Zweers MM, de Waart DR, Smit W *et al.* Growth factors VEGF and TGF-beta1 in peritoneal dialysis. *J Lab Clin Med* 1999; 134: 124–132
10. Saxena R. Pathogenesis and treatment of peritoneal membrane failure. *Pediatr Nephrol* 2008; 23: 695–703
11. Augustine T, Brown PW, Davies SD *et al.* Encapsulating peritoneal sclerosis: clinical significance and implications. *Nephron Clin Pract* 2009; 111: 149–154
12. Miyazaki M, Yuzawa Y. The role of peritoneal fibrosis in encapsulating peritoneal sclerosis. *Perit Dial Int* 2005; 25: 48–56
13. Schwartz SM. Smooth muscle migration in atherosclerosis and restenosis. *J Clin Invest* 1997; 100: 87–89
14. Amano M, Chihara K, Kimura K *et al.* Formation of actin stress fibers and focal adhesions enhanced by Rho-kinase. *Science* 1997; 275: 1308–1311
15. Olson MF. Applications for ROCK kinase inhibition. *Curr Opin Cell Biol* 2008; 20: 242–248
16. Nagatoya K, Moriyama T, Kawada N *et al.* Y-27632 prevents tubulointerstitial fibrosis in mouse kidneys with unilateral ureteral obstruction. *Kidney Int* 2002; 61: 1684–1695
17. Murata T, Arii S, Nakamura T *et al.* Inhibitory effect of Y-27632, a ROCK inhibitor, on progression of rat liver fibrosis in association with inactivation of hepatic stellate cells. *J Hepatol* 2001; 35: 474–481
18. Vargha R, Endemann M, Kratochwill K *et al.* Ex vivo reversal of in vivo transdifferentiation in mesothelial cells grown from peritoneal dialysate effluents. *Nephrol Dial Transplant* 2006; 21: 2943–2947
19. Margetts PJ, Bonniaud P, Liu L *et al.* Transient overexpression of TGF-beta1 induces epithelial messenchymal transition in the rodent peritoneum. *J Am Soc Nephrol* 2005; 16: 425–436
20. Patel S, Takagi KI, Suzuki J *et al.* RhoGTPase activation is a key step in renal epithelial mesenchymal transdifferentiation. *J Am Soc Nephrol* 2005; 16: 1977–1984
21. Mizukami Y, Fujiki K, Duerr EM *et al.* Hypoxic regulation of vascular endothelial growth factor through the induction of phosphatidylinositol 3-kinase/Rho/ROCK and c-Myc. *J Biol Chem* 2006; 281: 13957–13963
22. Kanda T, Wakino S, Hayashi K *et al.* Effect of fasudil on Rho-kinase and nephropathy in subtotally nephrectomized spontaneously hypertensive rats. *Kidney Int* 2003; 64: 2009–2019
23. Sasaki Y, Suzuki M, Hidaka H. The novel and specific Rho-kinase inhibitor (S)-(+)-2-methyl-1-[(4-methyl-5-isoquinoline)sulfonyl]-homopiperazine as a probing molecule for Rho-kinase-involved pathway. *Pharmacol Ther* 2002; 93: 225–232
24. Mondello S, Mazzon E, Di Paola R *et al.* Erythropoietin suppresses peritoneal fibrosis in rat experimental model. *Eur J Pharmacol* 2009; 604: 138–149
25. Riesenhuber A, Kasper DC, Vargha R *et al.* Quercetin protects human mesothelial cells against exposure to peritoneal dialysis fluid. *Pediatr Nephrol* 2007; 22: 1205–1208
26. Arbeiter K, Bidmon B, Endemann M *et al.* Peritoneal dialysate fluid composition determines heat shock protein expression patterns in human mesothelial cells. *Kidney Int* 2001; 60: 1930–1937
27. Bidmon B, Endemann M, Arbeiter K *et al.* Overexpression of HSP-72 confers cytoprotection in experimental peritoneal dialysis. *Kidney Int* 2004; 66: 2300–2307
28. Kanda T, Wakino S, Homma K *et al.* Rho-kinase as a molecular target for insulin resistance and hypertension. *FASEB J* 2006; 20: 169–171
29. Fusshoeller A. Histomorphological and functional changes of the peritoneal membrane during long-term peritoneal dialysis. *Pediatr Nephrol* 2008; 23: 19–25
30. Io H, Hamada C, Ro Y *et al.* Morphologic changes of peritoneum and expression of VEGF in encapsulated peritoneal sclerosis rat models. *Kidney Int* 2004; 65: 1927–1936
31. Hirahara I, Ogawa Y, Kusano E *et al.* Activation of matrix metalloproteinase-2 causes peritoneal injury during peritoneal dialysis in rats. *Nephrol Dial Transplant* 2004; 19: 1732–1741
32. Bozkurt D, Cetin P, Sipahi S *et al.* The effects of renin-angiotensin system inhibition on regression of encapsulating peritoneal sclerosis. *Perit Dial Int* 2008; 28: S38–S42
33. Suga H, Teraoka S, Ota K *et al.* Preventive effect of pirfenidone against experimental sclerosing peritonitis in rats. *Exp Toxicol Pathol* 1995; 47: 287–291
34. Miyata K, Shimokawa H, Kandabashi T *et al.* Rho-kinase is involved in macrophage-mediated formation of coronary vascular lesions in pigs in vivo. *Arterioscler Thromb Vasc Biol* 2000; 20: 2351–2358
35. Yanez-Mo M, Lara-Pezzl E, Selgas R *et al.* Peritoneal dialysis and epithelial-to-messenchymal transition of mesothelial cells. *N Engl J Med* 2003; 348: 403–413
36. Margetts PJ, Gyorffy S, Kolb M *et al.* Antiangiogenic and antifibrotic gene therapy in a chronic infusion model of peritoneal dialysis in rats. *J Am Soc Nephrol* 2002; 13: 721–728
37. Wakino S, Kanda T, Hayashi K. Rho/Rho kinase as a potential target for the treatment of renal disease. *Drug News Perspect* 2005; 18: 639–643
38. Masszi A, Di Ciano C, Sirokmány G *et al.* Central role for Rho in TGF-beta1-induced alpha-smooth muscle actin expression during epithelial-mesenchymal transition. *Am J Physiol Renal Physiol* 2003; 284: F911–F924
39. Kolosionek E, Savai R, Ghofrani HA *et al.* Expression and activity of phosphodiesterase isoforms during epithelial mesenchymal transition: the role of phosphodiesterase 4. *Mol Biol Cell* 2009; 20: 4751–4765
40. Cho HJ, Yoo J. Rho activation is required for transforming growth factor-beta-induced epithelial-mesenchymal transition in lens epithelial cells. *Cell Biol Int* 2007; 31: 1225–1230
41. Compton LA, Potash DA, Mundell NA *et al.* Transforming growth factor-beta induces loss of epithelial character and smooth muscle cell differentiation in epicardial cells. *Dev Dyn* 2006; 235: 82–93
42. Sugano N, Wakino S, Kanda T *et al.* T-type calcium channel blockade as a therapeutic strategy against renal injury in rats with subtotal nephrectomy. *Kidney Int* 2008; 73: 826–834
43. Aroeira LS, Aguilera A, Sánchez-Tomero JA *et al.* Epithelial to mesenchymal transition and peritoneal membrane failure in peritoneal dialysis patients: pathologic significance and potential therapeutic interventions. *J Am Soc Nephrol* 2007; 18: 2004–2013
44. Szeto CC, Wong TY, Lai KB *et al.* The role of vascular endothelial growth factor in peritoneal hyperpermeability during CAPD-related peritonitis. *Perit Dial Int* 2002; 22: 265–267
45. Aroeira LS, Aguilera A, Selgas R *et al.* Mesenchymal conversion of mesothelial cells as a mechanism responsible for high solute transport rate in peritoneal dialysis: role of vascular endothelial growth factor. *Am J Kidney Dis* 2005; 46: 938–948
46. van Nieuw Amerongen GP, Koolwijk P, Versteilen A *et al.* Involvement of RhoA/Rho kinase signaling in VEGF-induced endothelial cell migration and angiogenesis in vitro. *Arterioscler Thromb Vasc Biol* 2003; 23: 211–217

Received for publication: 31.12.09; Accepted in revised form: 4.1.11

特集 CKDとアディポサイエンス

◆臨床

肥満関連腎症の病態と治療

脇野 修　伊藤 裕

慶應義塾大学腎臓内分泌代謝内科

肥満にともなう腎障害は，肥満に合併する糖尿病および高血圧による腎障害と，肥満に固有の腎障害に分けられる．後者は組織学的には糸球体肥大と巣状分節状糸球体硬化症（focal segmental glomerulosclerosis: FSGS）を特徴としており，肥満関連腎症（obesity-related glomerulopathy: ORG）と言われている．ORGの発症機序には腎血行動態の異常，アディポサイトカインによる腎障害，インスリン抵抗性による腎障害などが想定されている．臨床的には肥満と慢性腎臓病（CKD）との関連を示す疫学データは多く報告されているが，外科的減量などの治療介入により直接的な因果関係を証明するデータはまだ乏しい．しかし，近年のCKD患者の増加に肥満人口の増加が寄与している可能性が指摘されており，従来の低蛋白食，減塩食，血糖管理，レニン-アンジオテンシン-アルドステロン系の抑制，血圧管理といったCKDの治療戦略に加え，肥満の病態管理もCKDの治療において重要になるものと思われる．

キーワード

肥満関連腎症（ORG），慢性腎臓病（CKD），アディポサイトカイン，インスリン抵抗性，脂肪毒性

はじめに

肥満にともなう腎障害には大きく分けて2つあり，一つは肥満に合併する糖尿病および高血圧による腎障害であり，もう一つは肥満に固有の腎障害である．これは組織学的には糸球体肥大と巣状分節状糸球体硬化症（focal segmental glomerulosclerosis: FSGS）を特徴としており，肥満関連腎症（obesity-related glomerulopathy: ORG）と言われている[1]．本稿ではORGの概念について紹介するとともに，慢性腎臓病（Chronic Kidney Disease: CKD）の危険因子としての肥満の意義および病態について述べる．

1 肥満関連腎症

Kambhamらは腎生検6,818症例中のBMI＞30の肥満71症例の解析を行った[2]．その結果，組織学的に糸球体肥大とFSGSを特徴とする病理所見が腎生検施行例の2％の頻度であることを見出した．そして1986年から2000年の15年間でその頻度が10倍に増加していること，原発性のFSGSと比較してネフローゼの頻度が低く，血清アルブミンのレベルは高く，血清コレステロールのレベルおよび浮腫の頻度は低いことなどが明らかとなり，ORGの疾患概念が確立された．現在，ORGは，①病的な肥満症（BMI＞40），②浮

腫を認めない蛋白尿，③正常血清アルブミン値の3つをtriadとし，高血圧による腎硬化症および糖尿病腎症を除外したものと定義される．蛋白尿はネフローゼレベルのものから0.5g以下の軽度のものまである．予後については，先述のKambhamらの報告によれば，8年間の観察期間で14％が血清クレアチニン値の倍加，3.6％で末期腎不全への進行が認められたという．またPragaらは，15名のORG患者のうち7名（46％）は腎障害が進行し，3名（34％）は血液透析に移行したと報告している[3]．このように，ORGの予後は必ずしも良いわけではないと考えられる．ORGの発症機序は後にも詳述するが，糸球体肥大については一酸化窒素（NO）の代謝障害による輸入細動脈の拡張，レニン-アンジオテンシン系（RAS）の活性化による輸出細動脈の収縮が，糸球体の過剰濾過を引き起こしていることが指摘されている．また肥満にともなう高インスリン血症がインスリン様成長因子（IGF）-1や-2といった成長因子の分泌を亢進させ，それが糸球体の肥大を引き起こすという報告もある．肥満における高レプチン血症がtransforming growth factor-β1（TGF-β1）の発現を誘導し，これが糸球体肥大を引き起こすとの報告もある．また原発性のFSGSの発症に腎臓内の虚血の存在が知られており，肥満にともなうことが多い睡眠時無呼吸症候群（SAS）による慢性的な腎臓の虚血がFSGSの原因とも考えられている．ただし，原発性のFSGSでは虚血に陥りやすい腎臓の皮質髄質の境界にsclerosisの病変が認められるのに対し，ORGではその傾向はないとされている．また近年，生後肥満になったりネフロン総数の少ない腎臓になる可能性が高い低出生体重児との関連も示唆されている．ネフロン数の減少に伴う腎病変はFSGSであることから，低出生体重がORGの根本原因ではないかとも考えられている[4]．

2 肥満と慢性腎臓病

近年新たな心血管病のリスクとして腎機能障害の存在が注目されてきている．腎機能の低下はそれが早期の段階であっても（たとえば微量アルブミンの段階）すでに心血管障害のリスクとなっていることが，多くの疫学データで証明されるようになってきた．その中で腎機能の評価，主としてGFR値に関して見直しがなされ，CKDの概念が提唱された．肥満は一部糖尿病，高血圧発症を介してCKDの原因となり，最終像として血液透析に至ると考えられるが，肥満そのものがORGという病態のもとCKDのリスクであるというデータも報告されている．長期の観察研究では，高血圧および糖尿病とは独立の危険因子としてBMIが指摘されている．Isekiらは BMIと末期腎不全の発症につき100,000人の日本人の集団につき17年間観察を続けた．その結果，BMIが増加するにつれて末期腎不全に移行するリスクが男性において高くなることが示された[5]．11,104名の大規模なコホートを用いて14年間観察した研究では，男性の肥満者でCKD発症のリスクが1.32倍高く，この関連は年齢，喫煙，運動量，アルコール摂取量，心筋梗塞の家族歴，糖尿病，高血圧，高コレステロール血症，冠動脈疾患との影響を除外しても認められた[6]．近年Wangらは，1980年から2006年に報告された247名の肥満と腎症に関する疫学調査のうち信頼性の高い25のコホート研究，3の横断研究，19の症例・対照研究を選びメタアナリシスを行った[7]．その結果，正常者（18.5＜BMI＜25）に比べ軽度肥満者（25＜BMI＜30）では腎疾患のリスクが高く，相対危険率が1.40であった．高度肥満者（BMI＞30）ではさらにリスクが高く，相対危険率は1.83であった．男女差があり女性の肥満者の相対危険率は1.92で，男

性では1.49であった．BMIと腎疾患発症の危険率は正の相関を示し，先進国の腎疾患において男性で13.8％，女性で24.9％がBMI 25以上の肥満に起因すると結論された．その一方で，BMIとCKDとの間にJ-shapeの関係を認める報告もある．すなわちやせの患者（BMI＜18.5）ではCKDのリスクが逆に正常者（18.5＜BMI＜25）と比べて高くなることも報告されている[8]．肥満とCKDとの間の直接的な因果関係については，正常血圧のIgA腎症，片腎の患者においては血圧に関係なく肥満が腎障害の危険因子となっていること，肥満（BMI＞30）の健常者からの移植腎はやせ（BMI＜25）の健常者からの移植腎と比べて障害が多いことからも関連が示唆されている．しかし，減量の介入試験が腎機能障害を正常化するか否かは十分証明されていない．わが国の研究ではBMI＞25の肥満患者12名を25kcal/kg体重の低カロリー食で減量させたところ，1年後に微量アルブミン尿が消失したという報告もある．近年，NavaneethanらはCKDにおける減量の効果についてメタアナリシスを報告している．13の前向き研究について解析がなされ，食事療法，運動療法，食欲抑制薬による非外科的減量により，平均7.4カ月の観察期間で蛋白尿の減少（－1.31g/日）と降圧が認められた．重度肥満に対するBariatric Surgeryによる減量では，半年から長期では13年の経過観察の症例検討が解析されており，過剰濾過によるGFRの上昇を低下させ，尿蛋白を減少させる効果が有意にあると結論されている[9]．すなわち，尿蛋白の減少については証明されているが，腎機能における減量の効果については否定的な報告もあり，いまだ議論の余地がある段階である．またBariatric Surgeryについては腎機能以外の長期の安全性については未知であり，今後の評価が必要である．

3 肥満に伴う腎障害の病理所見

先述のORGで認められる腎病理所見は，肥満に伴う糖代謝異常，高血圧，脂質代謝異常が関与し，病期としても尿蛋白がある程度認められる進行した腎障害を見ている可能性が高い．しかし，これらの合併症のない状態についての腎生検所見は，生検をする機会も少なく報告は少ない．この点についてReaらは腎障害のない肥満（BMI≧30，49名）および正常な腎移植ドナー（BMI＜30，42名）の腎生検所見を比較し検討している．その結果，尿細管腔の拡張，尿細管の空胞の減少以外は病理組織に変化が認められなかったとしている．肥満に伴う腎障害の初期の変化が，尿細管を中心とする障害であることは興味深い[10]．

4 肥満関連腎症の発症機序

先述のようにさまざまな因子が肥満に伴う腎障害の機序として想定されている．

1）アディポサイトカイン

脂肪組織から分泌されるサイトカイン（cytokine）すなわちアディポサイトカイン（adipocytokine）は，腎障害に対して重要な役割を有する．肥満の血圧調節，腎機能に関与するおもなアディポサイトカインには，アンジオテンシノーゲン，レプチン（leptin），アディポネクチン（adiponectin）などが挙げられる．レプチンの血中レベルは肥満において上昇し，摂食を減少させエネルギー消費を亢進させる作用を有する．レプチン受容体が腎臓において強く発現していることから，レプチンの腎臓における直接作用が想定されている．レプチンは培養糸球体内皮細胞においてTGF-βの発現を亢進させ，レプチンの持続注入モデルでは血圧に変化を来さずに蛋白

尿，糸球体硬化が認められた．以上からレプチンは肥満関連腎症の発症因子の一つであると考えられている．さらに近年，アディポネクチンの腎臓における意義が明らかとなった．アディポネクチンの作用はインスリン感受性の亢進，抗炎症，抗動脈硬化作用などである．肥満，糖尿病，インスリン抵抗性状態においてはその血中レベルが低下することが知られている．アディポネクチン欠損マウスでは腎臓のポドサイトの足突起の融合が認められ，アルブミン尿が認められた．そして，アディポネクチン欠損マウスにアディポネクチンを補充すると，病理組織の正常化およびアルブミン尿の改善が認められた[11]．アディポネクチンの低下が，肥満における腎障害の機序を説明する新たな因子として注目されている．

2）腎細胞内の脂肪蓄積

脂肪そのものが腎細胞，尿細管細胞，メサンギウム細胞，内皮細胞に障害を引き起こすことが知られている．これを腎臓における lipotoxicity という．肥満における内臓脂肪の蓄積は，遊離脂肪酸の血中レベルを上昇させる．この遊離脂肪酸は細胞内でミトコンドリアに取り込まれ，β-酸化に利用される．肥満においてはそのミトコンドリアにおける遊離脂肪酸の取り込みが低下する．そのため，細胞内に蓄積する脂肪酸およびその代謝産物（Diacylglycerol，Fatty acyl CoA，Ceramide）などがProtein kinase C，NF-κBを活性化し，炎症や細胞死を引き起こす[12]．Leviらのグループは脂肪酸やコレステロール生合成のmaster geneであるSREBP（Sterol-regulatory element binding protein）の発現が亢進していることが，肥満による腎臓のlipotoxicityの原因であるとしている．SREBPは転写因子でSREBP-1a，SREBP-1c，SREBP-2に分類され，SREBP-1は細胞内の脂肪酸合成に，SREBP-2はコレステロール合成に関与する．

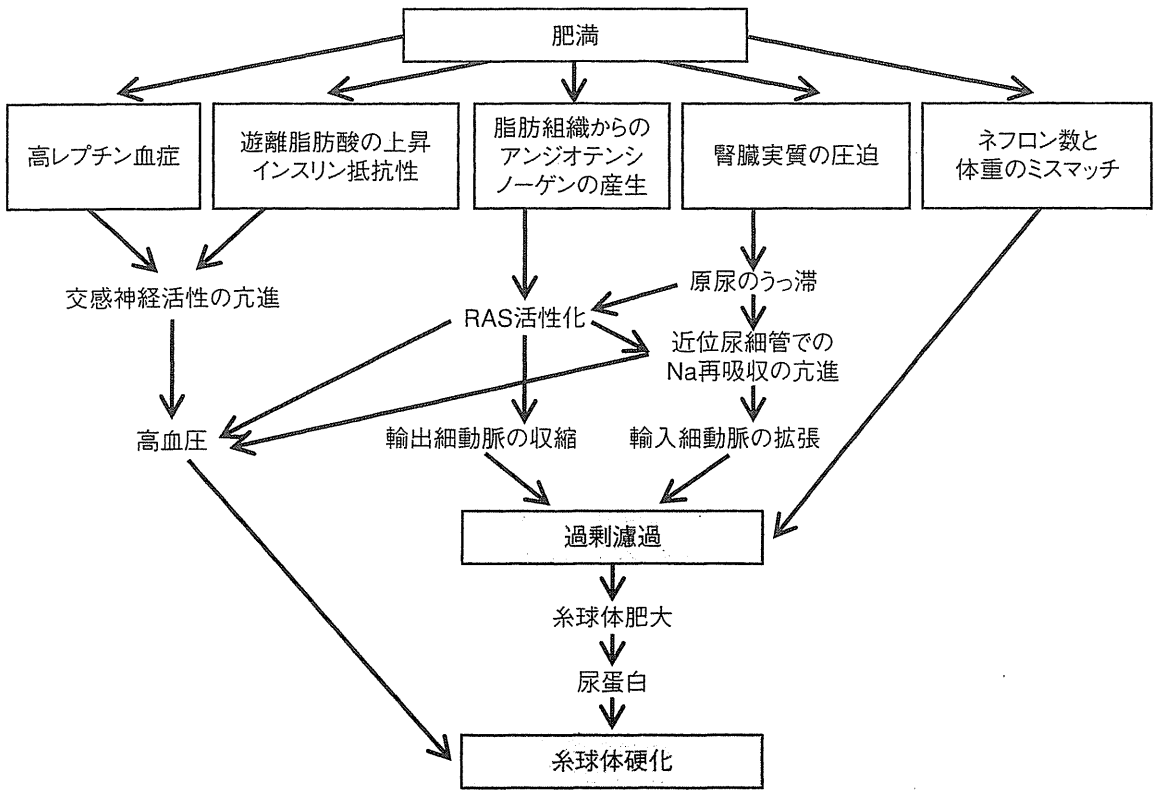

図1　肥満症における腎血行動態 RAS: renin-angiotensin system

肥満者の腎臓ではこれら転写因子の発現が亢進し，細胞内にlipidが蓄積し，細胞障害に働くことを報告している[13]．さらに脂質異常が腎機能に及ぼす影響について，TG-rich lipoproteinの腎毒性が指摘されている．VLDLおよびLDL受容体がメサンギウム細胞に発現しており，メサンギウム細胞の増殖，TGF-βの発現亢進を引き起こすことが報告されている．またアルブミンに結合している遊離脂肪酸（albumin-saturated free fatty acid）の尿細管細胞障害も指摘されている．アルブミン尿中に存在する遊離脂肪酸は脂溶性であり，細胞膜を通過して細胞障害や炎症を引き起こすことが報告されている[14]．

3）腎血行動態の異常

肥満特有の血行動態が腎症を引き起こす一つの因子となっている可能性が示唆されている．肥満の患者は交感神経活性の亢進，Na再吸収の亢進，RASの亢進等により難治性の高血圧を来しやすい．この高血圧が腎障害を引き起こす．さらに糸球体の過剰濾過も腎症進行の危険因子となっている．その原因としてRAS系の亢進，ネフロン数の低下のほかに，内臓脂肪組織増加にともなう腎臓実質の圧迫が挙げられる[14]（**図1**）．内臓脂肪の増加は先述のアディポサイトカインの発現異常にも関連するため，高血圧，eGFRはBMIよりも内臓脂肪量すなわちウエスト・ヒップ比，腹囲径によく相関することが示されている[15]．我々は内臓脂肪のなかでも特に腎周囲の脂肪組織の意義に注目している．以前より内臓脂肪の除去によりラットの寿命延長が認められることが報告されている[16]．現在，腎周囲脂肪組織の除去が肥満関連腎症の改善につながるかどうかを検討している．

4）インスリン抵抗性および高インスリン血症

肥満の主要な病態としてインスリン抵抗性，高インスリン血症が挙げられる．肥満では腎臓のインスリン感受性が保たれており，

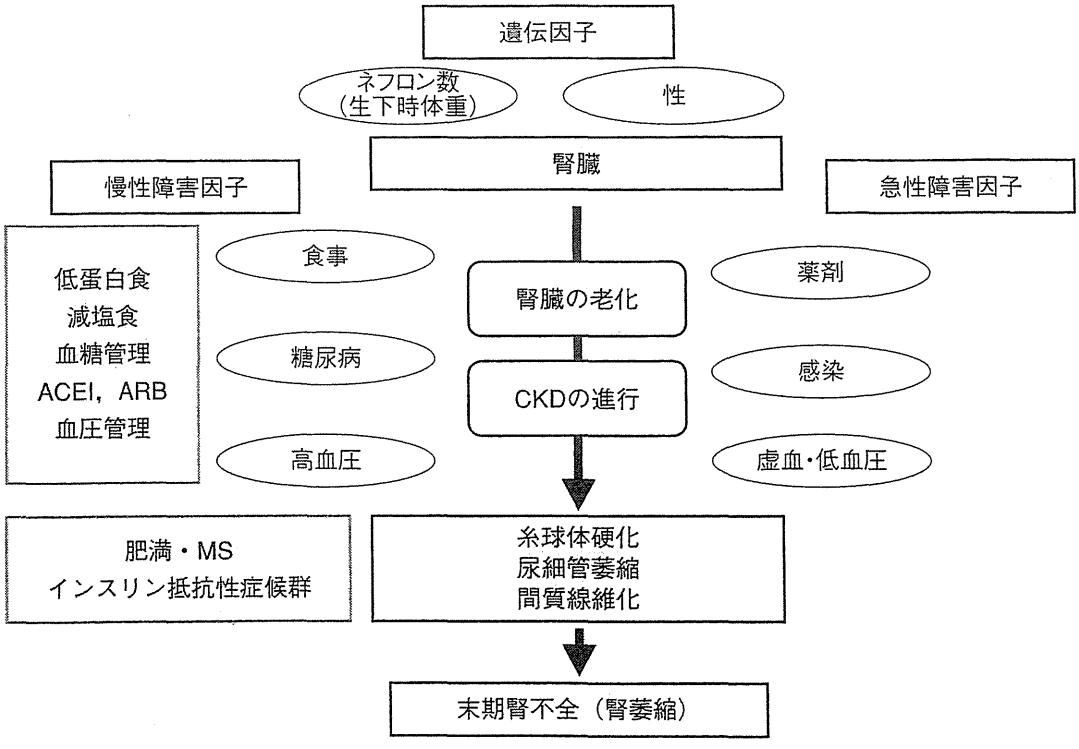

図2 CKDの進展

ACEI: ACE阻害薬，MS: メタボリックシンドローム